Ca' Foscari University of Venice

Master's Degree

in

Environmental Sciences

LM-75

Final Thesis

RECONSTRUCTING FIRE HISTORY FROM 1700 TO PRESENT THROUGH THE ANALYSIS OF ORGANIC COMPOUNDS IN SPELEOTHEMS: A HIGH RESOLUTION STUDY FROM NORTHWESTERN AUSTRALIA

Supervisor
Prof. Carlo Barbante

Assistant supervisor
Dr. Elena Argiriadis

Graduand
Giulia Genuzio
Matricolation number: 875231

Academic Year
2019 / 2020

Contents

ABSTRACT

Wildfires are very suggestive phenomena, even though they pose a serious threat to society. Australia is an example of how humans have to deal with extreme fires in terms of safety measures and prediction of future events. Therefore, it is crucial to improve the knowledge of bushfires so as to increase people's readiness and reduce economic and ecological losses.

Reconstructing the history of fires reveals whether and how the frequency and intensity of events has changed over time providing information about past climates and vegetation. This knowledge is of considerable value for more accurate predictions of future fire events.

The aim of the current research work is to reconstruct fire history from stalagmites, by investigating organic compounds that are excellent indicators of fire and environmental change. An innovative analytical methodology was applied since the concentration of analytes preserved in the stalagmite is extremely low. The analysis of polycyclic aromatic hydrocarbons stored in a stalagmite is able to discriminate whether they were originated by combustion and thus are suitable for the reconstruction of paleo fires in northwestern Australia. The further analysis of *n*-alkanes provides information on the type of vegetation present above the cave as these molecules are proxies of vegetation cover. The work requires the preparation of samples by drilling, acid digestion, liquid-liquid extraction and concentration in organic clean room. Very rigorous decontamination procedures were followed to minimize sample contamination and increase the analytical signal. The analyses were performed by gas chromatography combined with single and triple quadrupole mass spectrometry. The expected results will enable the evaluation of past fires in terms of intensity, frequency and type of vegetation affected in the last three centuries.

1. INTRODUCTION

1.1 FIRES IN AUSTRALIA

1.1.1 Fire as climate driver

Fires are certainly one of the most fascinating and dangerous events of our planet. They represent a threat to societies in terms of human lives and economic loss; their impacts extend to vegetation, fauna and soil [1]. Therefore, it is crucial to enhance knowledge of these phenomena so to predict future events, increase population preparedness and minimize damages.

After all these considerations, a natural question arises: are fires always harmful events? How did life on Earth adapt to these phenomena?

The answer to this question requires a wider point of view: the ecosystem approach. Bushfires are one of the most important drivers of biodiversity in ecosystems such as chaparral and savannah: they release a huge amount of energy in a very short time making stored resources and nutrients available again. This causes an increase in species richness and a wider spatial heterogeneity. Fires play a key role in these ecosystems because they keep disturbance at an intermediate level that maximizes ecosystem biodiversity and productivity [2].

Understanding fire patterns is complex because each event is characterized by different intensity, size, frequency, temporal and spatial scale. Furthermore, it is essential to consider factors involved in fuel typology and fire spreading such as vegetation type and structure, amount of rainfall, soil texture and topography [3].

1.1.2 Importance and role of fires in Australia

One of the most suitable places to study fire events is the Australian continent. Bushfires are so frequent and extended that authorities have established an alert system to prepare citizens in case of imminent danger. A reason why this territory is so vulnerable to these phenomena is the combination of climatic conditions and vegetation cover. Since the aim of this thesis is to analyze paleofires, a short general description of Australian climatic conditions is provided.

Aridity is present in most of the continent with few exceptions of temperate zones in Southeast and Southwest. Northern Australia presents a tropical climate and it is influenced by monsoonal activity. Here, a wet season of four-five months alternates to a dry season [2]. Plants are adapted to survive dry periods, indeed the dominant type of vegetation is hummock grassland. Eucalypt and acacia forests as well as woodland with understory and also treeless and shrub lands are found in eastern and Northern Australia [4]. In this context, the chances to trigger a bushfire are high during all year, in every part of the continent. The last ingredient to take into consideration is local weather. The fire season includes climate, vegetation and weather conditions so to determine the peak of burning activity in a specific region. Since weather varies with seasonality, the peak of chances to ignite a bushfire is different across the continent and during the year [5].

Figure 1.1. Fire seasons in Australia [5].

The map in Figure 1.1 shows how peak burning activity affects each climate zone in different periods of the year. Northern Australia is affected the most during winter and spring (June-November).

The influence of weather can be explained through this simple mechanism. Vegetation rapidly grows during the wet season so dead matter accumulates on soil. This matter dries out during the hot season becoming a potential fuel. These

are the best circumstances for a fire to start. The presence of a dry wind will increase the speed of spreading. Fire frequency is mainly affected by vegetation structure and amount of rainfall. As a matter of fact, the shortest fire intervals occur in case of grassland (intermediate productivity) and intermediate level of rain [5, 2].

1.1.3 Importance of reconstructing past fires

Understanding the nature and the propagation mechanism of fires is becoming a vital issue to prevent startling consequences as the ones happened in Australia in January 2020. Despite society preparedness, the country is facing a dramatic scenario known as Black Summer Bushfires. The fire season started in spring (November 2019) in Southern territories and it swept through more than seven millions hectares massacring billions of animals, leading threatened plants towards extinction, burning thousands of houses and causing thirty-four people to pass away [6].

Scientists from all over the world are trying to investigate this extreme phenomenon. One method is based on climate models: they are effective tools that integrate greenhouse gases emissions with weather conditions and vegetation cover to simulate the potential risk of bushfires. Even if results show an increment of 30% in fire probability, scientists do not fully rely on models because they underestimate the influence of anthropogenic greenhouse gases and the amount of heat released during an extreme fire event. Moreover, models are not able to predict unheard-of scenarios like the one happened this year [6]. However, Australian observations show a steep increment in fire risk in the last century, which is likely to increase further in the future. Improving society preparation is a key step but it is not enough because unprecedented events may occur [6]. Therefore, a broader knowledge of fires is needed.

A way to get a deeper insight into fire regimes and mechanisms is the reconstruction of past climate events. Fire history provides details on how

bushfires changed over time, circumstances and frequency of past extreme events, climatic conditions and type of vegetation affected. All this information is extremely important to address the current situation and to predict future scenarios more accurately.

Figure 1.2. Fire warning indicates the risk of catastrophic bushfire events [7].

1.2 HOW TO RECONSTRUCT PAST FIRES

1.2.1 Proxies and archives

Climatologists use different methods to reconstruct the climatic history of the planet. The main sources of past information are recorded in archives such as corals, tree rings, ice cores and sediments. Reading the history preserved in archives is far from being simple, since numerous factors might interfere during the signal incorporation in archives affecting resolution, continuity and quality of records. Marine sediments, for example, might be eroded by wave action after being deposited, then transported by currents and re-deposited elsewhere. Changes in sea level affect deposition rates as well as corrosive waters alter sediments. As a consequence, the resolution of archives depends on disturbances caused by processes that happened after the initial deposition and the interval of time needed to bury records and preserve them from future interferences [8].

Paleoclimatology focuses on natural phenomena that are highly dependent on climate variability and therefore provide a climate proxy record. Climate proxies are physical, chemical or biological characteristics preserved by the environment that replace a direct measure of climate variability [9]. Thus, they are excellent tools to reconstruct past events because they work as indirect measures of climate-dependent phenomena or climatic signals.

Examples of biological proxies are pollen assemblages deposited in lake sediments. The pollen is produced by the surrounding vegetation and transported by the wind to oxygen-depleted lakes where it is deposited. Their relative abundance, absolute concentration and type reveal information about the main vegetation type and further details about climate-sensitive species (e.g. spruce indicates cold temperatures). To increase the accuracy of the reconstruction, it is necessary to compare pollen assemblages with other fossils such as seeds and cones that cannot be transported very far from their origin [8].

Ice cores contain many geochemical proxies. The analysis of the air stored inside the ice reveals ancient greenhouse gases concentrations while the isotopic composition of oxygen and hydrogen is a proxy of temperature. Ice cores detect

variations in the thickness of the deposited snow, which is related to humidity and air temperature. In addition, dust particles in ice cores are essential to reconstruct wind circulation [7].

Biomarkers are crucial molecular proxies because they reveal information about the processes that originated them. In particular, fire biomarkers are molecules that are very resistant to transport and biodegradation so they are useful to reconstruct important features of fires such as intensity and combustion temperature [9, 11]. Since this research work uses fire biomarkers, a more detailed description of this category of proxies is provided in the next pages.

Figure 1.3. Examples of archives used in Paleoclimatology [12].

This general overview highlights the variety of archives and proxies that are combined by scientists to reconstruct the climatic history far beyond the time covered by direct measurements. Therefore, understanding how the climatic signal was recorded and which are the potential interferences is crucial to correctly interpret the climatic information. Once the signal has been identified, it is necessary to match it to a timeframe and calibrate it [9].

Calibration is a procedure that relates the proxy to a modern climate record and it determines the degree of climate-dependency of the proxy. This method is based on the "principle of uniformitarianism" according to which current and past environmental phenomena present similar natural mechanisms and dynamics. Therefore, it is important to improve knowledge of modern processes to be able to

reconstruct paleo events more accurately. However, when current and past conditions are very dissimilar, the principle is no longer applicable.

However, merging information stored in different archives is complex because proxies are various in terms of spatial-temporal scale, resolution and recorded signal [8]. For instance, abrupt changes in climate are not always easy to detect in proxies. The presence of a lag between a sudden climatic change and the recording phenomenon causes a gradual transition in the proxy where it is difficult to identify the abrupt change. Another important aspect is that the climatic signal may not be recorded continuously, affecting the resolution of the record.

In any case, the most important tool for a precise paleoclimatic reconstruction is accurate dating. In fact, it allows to define a chronological order of past phenomena and their potential temporal lag (inertia) so to better understand how climate forcing has acted in the past [13]. This is possible because when a dating method does not provide an absolute age, it is still possible to detect the relative age of a series of samples. Dating methods are divided in four general categories: radioisotopic methods, paleomagnetic methods, chemical methods and biological methods.

1.2.3 Radioisotopic dating

Isotopes are atoms of the same element that differ in the number of neutrons (while maintaining the same atomic number). Many elements have different types of isotopes: some of them are not stable and undergo the process of radioactive decay, which is the basis of the radioisotopic dating method.

In few words, radioactive decay occurs when an initial unstable isotope (parent isotope) in the archive is transformed into a more stable isotope (daughter isotope) by losing the α and β particles. The rate of transformation is measured by the half-life: the amount of time needed to convert half the initial concentration of the

parent isotope into a daughter isotope [7, 8]. Therefore, in the case of closed system archives, it is easy to determine the precise age if the initial concentration of the parent isotope is known. Basaltic rocks are an example of such archives: they are formed by a rapid cooling of lava and their structure does not allow any isotope exchange with the external environment. Decay rates are various depending on elements, so long half-lives (i.e. uranium to lead) are chosen to date rocks as old as the planet Earth whereas shorter ones (i.e. potassium to argon) are used in dating younger sediments [8].

However, there are some constraints to the application of this dating method. As already mentioned, the initial concentration of the parent isotope must be known, so it must be present in a measurable amount. In addition, the half-life of the parent isotope must be known and it must be suitable for the time span of the archive to be dated. Furthermore, there must be a connection between a dated phenomenon and the beginning of radioactive decay [13].

Among the different types of radioisotopic methods, the most commonly used to date speleothems is the uranium decay series. This method consists in measuring the balance between chemical species of a chain of radioactive decay and it allows to date archives up to few hundred thousand years ago.

In the uranium-series, the parent isotope is uranium-238, which decays into a series of unstable nuclides before being converted to its last stable isotope, lead-206. The most relevant for dating are the isotopes: ^{238}U, ^{234}U and the daughter isotope ^{230}Th [13]. The first two are sometimes found in the archives as calcium substitutes. Since uranium is not stable, it slowly decays into its daughter isotope thorium. The latter is also not stable and it is therefore converted into other nuclides with a half-life of 75,000 years. The first conversion (from uranium to thorium) occurs very slowly compared to the second one (thorium to other nuclides). The amounts of uranium and thorium in the archive reflect the slow decay of the parent isotope and the rapid conversion of the daughter isotope to other nuclides. It is precisely on the Th/U ratio that this dating method is based and it allows scientists to date archives up to one hundred thousand years ago [8].

This methodology is very effective in the case of undisturbed closed system archives, which is why it is widely applied to speleothems. In fact, the percolation of thorium in the cave is hindered by its low solubility in surface water, thus preventing external contamination. The precise determination of the initial parental isotope concentration is essential to distinguish whether thorium has formed from the decay of uranium within the archive or whether it has an external origin [14].

1.2.4 Fire biomarkers

As climatic history, the reconstruction of past fire events is based on information stored in archives and proxies. To better understand how these analyses are carried out, it is essential to get back to the starting point: the combustion process.
Combustion is an exothermic reaction that involves two reactants (fuel and oxygen) and ignition; the latter is a necessary component to start the process. Products are various depending on many factors such as the type of fuel, the amount of heat released, flame temperature, reaction progress. Through the analysis of the properties of combustion products, scientists collect information on fuel typology and on how the reaction occurred. Some of these organic molecules are called “biomarkers” because they perform as fire proxies. In fact, they are very resistant to processes such as biodegradation or transport. Since they maintain their molecular structure unchanged, it is possible to trace their source and, in certain cases, to distinguish whether their origin is linked to human activities or natural events. Fire biomarkers are numerous and have very different characteristics. They are usually transported by the wind: the distance from their source varies depending on the type of molecule. In addition, there are various types of biomarkers: depending on their characteristics they reveal information about the different features of fires. Therefore, the combination of different biomarkers is essential for accurate analysis.
For instance, charcoal originates from the combustion of woody vegetation. Since these particles can be carried by the wind only for few kilometers from their

origin, they are good indicators of local fires. However, charcoal does not reveal the intensity of the event [10]. A molecular marker of fire is levoglucosan: it originates from the combustion of cellulose and it is used to detect the intensity of fire. Differently from charcoal, it can be transported over long distances, even hundreds of kilometers [9, 15].

Since this research focuses on PAHs and alkanes stored in speleothems, a more comprehensive description of these fire proxies is now provided.

1.2.5 Polycyclic aromatic hydrocarbons (PAHs)

Polycyclic aromatic hydrocarbons (PAHs) are organic molecules composed of hydrogen and carbon atoms that form two or more fused aromatic rings. The stability of these compounds is related to the low H:C ratio. PAHs are carcinogenic and mutagenic since their peculiar structure matches the DNA perfectly, altering its functionality. Carcinogenicity increases with increasing molecular weight. Because of their harmfulness, the United States Agency for Toxic Substances and the Register of Diseases has established a priority risk list of 17 PAHs. The listed compounds are the most dangerous to human health among PAHs, they are present in the highest concentrations and they are those to which people are potentially most exposed [13, 14].

They are mainly produced by the incomplete combustion of organic matter occurring under conditions of oxygen deficiency. The chemical reactions that form PAHs are pyrosynthesis and pyrolysis. Among the most widely used fuels that form PAHs are coal, oil and tar. Other sources of these molecules are biodegradation by fungi and bacteria, volcanic eruptions, tobacco smoke, car exhausts and fires [16, 18]. They are usually present in nature as a mixture of different compounds. PAHs can also be synthesized in the laboratory and used as components of pesticides, plastics and asphalt [17]. Biomass burning, one of the main natural sources of PAHs, is considered in this work. This process occurs very quickly and at high temperatures, releasing an enormous amount of energy. When biomass heats up, it losses water and is hydrolyzed and oxidized. At this

point, pyrolysis begins, generating coal, tar and gaseous compounds.

The actual combustion starts when tar and gases reach the ignition temperature and flames are released as long as there are flammable substances, generating water vapor, inorganic and organic products. When flames are extinguished, smoldering begins, which can last several days. PAHs and other organic compounds are formed during both flaming and smoldering. Wildfires generate qualitatively and quantitatively different products depending on the type of fuel, predominance of flaming or smoldering phase, humidity and temperature conditions. Analyzing combustion products is critical to understand which type of vegetation was affected by the fire, since for instance, combustion of a meadow produces compounds very different from those of a tropical forest [19].

According to their molecular weight, PAHs are present in different forms. Molecules containing one to three aromatic rings are gaseous, while three to five are water insoluble and present both in vapor and particulate phases (phase partition is related to atmospheric temperature). PAHs with more than five aromatic rings are usually hydrophobic and adsorbed on aerosol particles. The transport of these molecules depends on their molecular weight. Gaseous PAHs are easily dispersed, while high-molecular-weight PAHs are first adsorbed on airborne particles and then scavenged by precipitation [18, 16].

PAHs are excellent fire proxies because their chemical structure is an indicator of combustion temperature. PAHs are formed in conditions of oxygen deficiency, at temperatures between 300 and 600 °C but their crucial characteristic is the increase in the number of aromatic rings as the combustion temperature increases. This specific characteristic, together with their high stability and persistence in the environment, makes these aromatic molecules excellent fire biomarkers. In fact, knowing the concentration and type of PAHs, it is possible to trace combustion temperature and fire intensity [11].

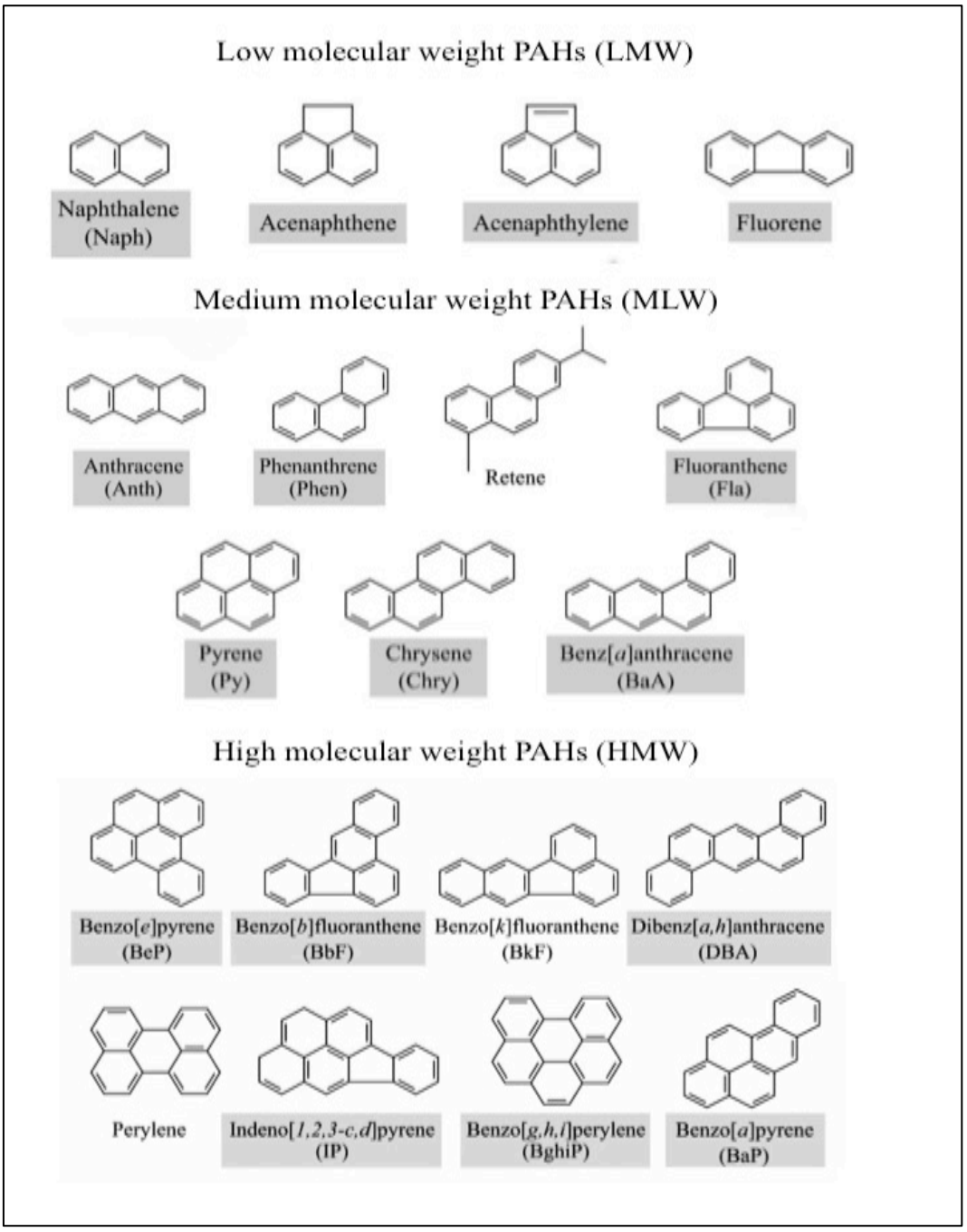

Figure 1.4. PAHs present in the current study. Elaborated from [20].

1.2.6 *n*-Alkanes

Alkanes are molecules composed of hydrogen and carbon atoms and they are known as saturated hydrocarbons because they have only single bonds. Their structure can be branched or unbranched and their general formula is C_nH_{2n+2} [20]. The prefix "*n*-" in *n*-alkanes stands for "normal" which means a straight-chained molecule. They are insoluble in water because of their non-polar covalent bond between carbon and hydrogen atoms and since their density is lower than water, they float on it. Moreover, they are characterized by a low boiling point (for same molecular weight) and very low reactivity, with the exception of combustion (they are among the most widely used fuels).

Alkanes are gases, liquids or solids depending on the number of carbon atoms contained in the molecule. Low-molecular-weight alkanes (1 to 4 carbon atoms) are gases; 5 to 17 carbon atoms are liquids. The last group consists of high-molecular-weight alkanes (over 18 carbon atoms), which are solid and include plant waxes [21]. The latter are some of the constituents of the cuticle, an outer layer that covers leaves and fruits and keeps the moisture constant. Terrestrial plants synthesize *n*-alkanes with a higher prevalence of odd chains than even ones, whose average length is 25-35 carbon atoms [22].

In this research, alkanes were chosen as a proxy because their molecular structure is highly resistant to biodegradation due to their low reactivity. This characteristic makes *n*-alkanes excellent biomarkers because these molecules remain intact both during transport into the cave and after deposition in the archives. The length of the chain reveals important details about the vegetation above the cave. Higher plants usually have waxes that are very resistant to biological degradation and characterized by high-molecular-weight *n*-alkanes. Furthermore, high concomitant concentrations of C_{25} and C_{27} reveal the presence of microbial activity associated with forests and woodland vegetation, while grasses and pastures are mainly characterized by the abundance of C_{31}. Angiosperms produce more *n*-alkanes than gymnosperms (both evergreen and deciduous). Low-

molecular-weight *n*-alkanes, on the other hand, are more indicative of the activities of bacteria, fungi and algae [10, 50, 25].

However, several factors can alter the abundance of *n*-alkanes in the archives. They may be produced from other sources such as bacteria, algae or fungi, which may also have contributed to biodegradation [22]. In addition, soil type influences the conservation of these biomarkers: alkaline soils are more abundant in *n*-alkanes than others with lower pH [25].

Anyway, these biomarkers are crucial to reconstruct past vegetation cover and land use changes. In fact, they are able to detect agricultural activities providing insights on the presence of humans and their influence on the surrounding environment [26].

1.3 SPELEOTHEMS

1.3.1 Formation

Speleothems are chemically precipitated deposits of calcium carbonate whose formation occurs when the groundwater percolates into a cave and evaporation or degassing facilitate the deposition process [27].

Various shapes develop in the limestone cave as a result of the location and rate of deposition: stalactites and stalagmites certainly are the most common formations. Stalactites are long vertical structures hanging from the ceiling of the cave that are internally hollow. The growth develops around the central core and the vertical component is more pronounced than width [28]. Stalagmites grow continuously upward at the bottom of the cave, below a drip-point and they present a compact structure. Similarly, flowstones consist of an overlapping of depositional layers that takes place beneath flowing water films. The reason why the paleoclimatic reconstruction is mainly focused on the analysis of stalagmites and flowstones lies on their laminated and solid structures able to conserve a variety of environmental proxies. Indeed, stalactites are less reliable archives because their growth might be not coherent since it can be impeded by obstructions in the empty core [27].

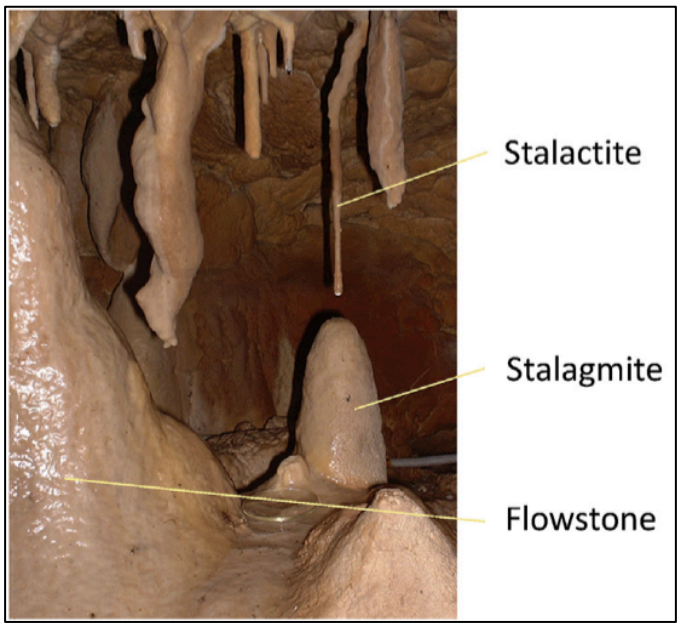

Figure 1.4. Examples of speleothems [10].

The precipitation of calcium carbonate generates two crystal forms: calcite and aragonite, which are the main components of speleothems. Since their formation is related to the karstic phenomenon, a brief description of its characteristics is provided.

1.3.2 The karstic phenomenon

Karst occurs when meteoric water dissolves the carbonate bedrock (typically limestone) and it percolates deep down underground. The dissolution process takes place because biotic activity produces carbonic acid, which reacts with the carbonate rock. The karstic phenomenon can also happen in presence of various types of bedrocks so speleothems can consist of different minerals. Karstic cavities present a vast variety of dimensions (from few millimeters to kilometers) and a widespread geographic distribution because of the variability of factors involved [13, 14].

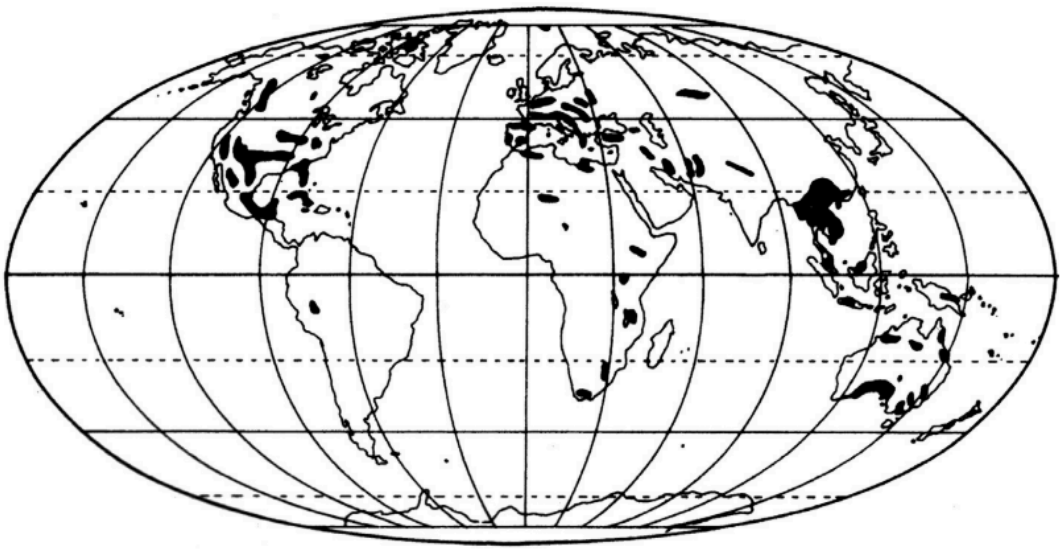

Figure 1.5. Worldwide distribution of karstic landscapes [11].

The karstic process starts at the surface where meteoric water is at direct contact with atmospheric CO_2. During its downward transport, water flows over different substrates that might change its chemical properties. When water is at contact with soil, it is enriched with soil gases and biotic CO_2; consequently, the partial pressure of CO_2 increases. As percolation continues, water flows over the bedrock: dissolution takes place only in presence of soluble rocks such as calcite, aragonite or dolomite. As the water reaches the entrance of the cave, evaporation begins to increase the concentration of Ca^{2+} until the solution is supersaturated with $CaCO_3$, causing the deposition of carbonate crystals and the formation of speleothems in the deepest parts of the cave.

As the name suggests, the precipitation zone is characterized by the precipitation process, caused by the degassing of CO_2. The precipitation rate is subject to seasonal fluctuations due to external and internal conditions of the cave. The concentration of CO_2 is related to both the quantity and chemistry of the raindrops and the conditions of air circulation in the cave [30].

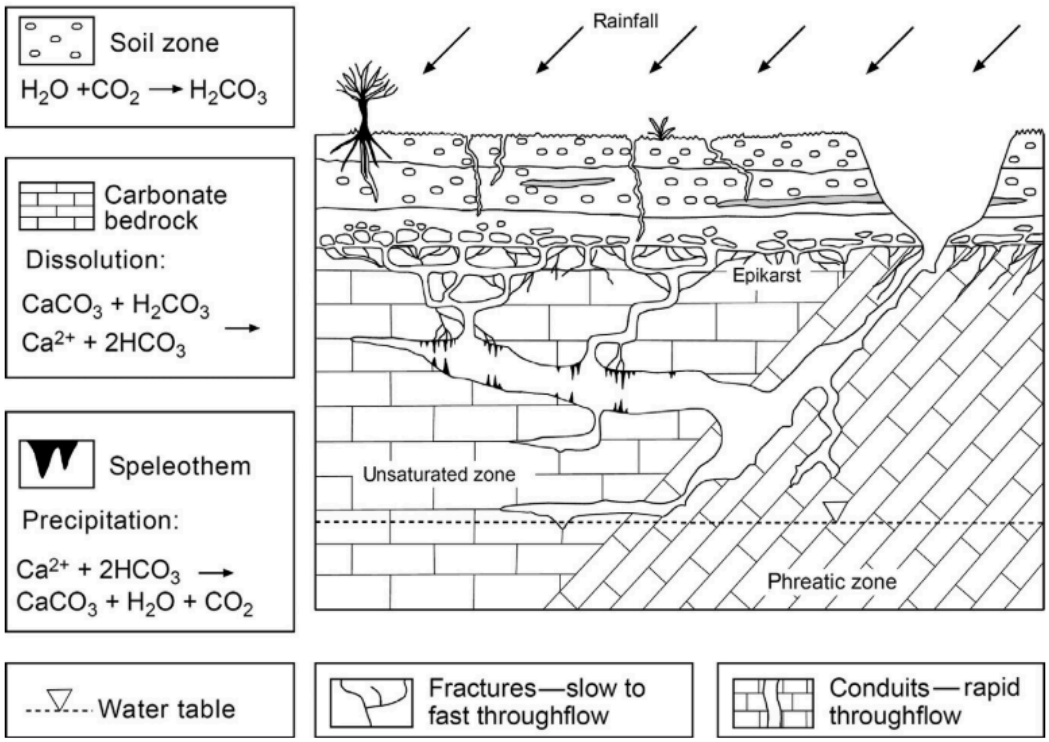

Figure 1.6. The cave system: dissolution and deposition processes [11].

This process occurs as a result of the different partial pressure of CO_2 between the percolated water and the surrounding cave environment. The outgassing of CO_2 increases the concentration of dissolved calcite: the deposition of calcium carbonate begins when the solution is supersaturated, forming speleothems [24, 25].

Figure 1.7. Stalagmites growing in Grotta Gigante cave, in Trieste (Italy).

1.3.4 How to date speleothems

Speleothems are mainly dated using uranium series. As mentioned above, uranium-238 decays to daughter isotopes. The separation between parent isotope and daughter species occurs before the precipitation of calcium carbonate and it is a natural process. In fact, the former isotope is soluble in water while thorium and palladium (daughter species) are not. Thus, the amount of the latter species in speleothems is very scarce. Dating of stalagmites and flowstones is highly reliable because they are closed systems and thorium content is derived exclusively from uranium decay. In fact, since thorium is extremely poorly soluble, external contamination is severely impeded. The accuracy of this method is ultimately dependent on an initial precise measuring of $^{234}U/^{238}U$ to exclude potential external contamination of thorium.

Last but not least, calcium carbonate crystals are very large in size and have a low tendency to recrystallize, which makes them very suitable for this dating technique [31].

1.3.5 Speleothems and Paleoclimatology

The crystallization process may include elements other than calcium carbonate, such as uranium, organic matter and molecular markers. While some of them are absorbed on the surface of the crystal, others are dissolved. Analyzing these additional elements and molecules reveals essential information to reconstruct past climates, plant cover and discrete events (such as fires or floods). Among the several terrestrial archives, speleothems are used in paleoclimatology because they form under stable conditions characterized by an almost constant temperature and a stable concentration of CO_2. Their continuous growth shapes laminated structures that preserve information about the surrounding environment. More precisely, speleothems are able to record variations inside the cave caused by external climate changes [30]. Therefore, the present work aims to reconstruct the history of fires occurred from 1700 to the present day through the analysis of fire biomarkers such as PAHs and *n*-alkanes.

1.3.6 Other proxies

Speleothems store several proxies. These include oxygen isotopes that are good indicators of humidity and rainfall and carbon isotopes that reveal variations in soil type, vegetation and moisture. The analysis of percolation water is crucial because this water has been in direct contact with the overlying environment and it transfers valuable information on climate and isotopic composition of oxygen and carbon to the layered structures of speleothems.

Oxygen isotopes are widely used for the reconstruction of paleotemperatures because their isotopic composition is highly temperature-dependent for two different reasons. First, the isotopic composition of oxygen in raindrops depends on temperature. Secondly, the oxygen isotopic fractionation that occurs during the crystallization process of calcite is also temperature dependent. Since stalagmites are formed in isotopic equilibrium with drip water, it is possible to reconstruct past surface temperatures over the entire growth period by analyzing the $^{18}O/^{16}O$ ratio stored in $CaCO_3$ crystals. Moreover, $\delta^{18}O$ found in stalagmites is an excellent tracer of variations in the intensity of monsoonal activity because it depends on the isotopic composition of meteoric water [29, 52].

As for oxygen, the isotopic composition of carbon stored in calcite provides information on the origins of this element. Carbon may derive from soil, atmospheric carbon dioxide or the oxidation of organic matter. The analysis of the $^{13}C/^{12}C$ ratio enables the reconstruction of changes in the vegetation above the cave. In fact, two main mechanisms are causing $\delta^{13}C$ variations and both are affected by climate change. The first one is observed when the $\delta^{13}C$ value increases because the composition of the vegetation changes: there is an increase of C_4 plants compared to C_3 due to a transition from forest to grassland. In the second case, a change in vegetation density causes a variation in $\delta^{13}C$ value. High values of $\delta^{13}C$ are found on the bare soil because the dissolution of limestone occurs through water in direct contact with atmospheric CO_2. On the contrary, the presence of vegetation reduces the value of $\delta^{13}C$ because the dissolution occurs with water that refills the plants. The dynamics determining the $^{13}C/^{12}C$ ratio are

very complex and require further investigation. In fact, the precipitation of calcite itself may play an important role in the alteration of $\delta^{13}C$ value [29].

1.4 ORGANIC MATTER IN SPELEOTHEMS

During the formation and growth of speleothems, organic matter may be incorporated between the layers, providing precious information about past climates. This process occurs during the precipitation of calcium carbonate crystals by adsorption onto the surface of the crystals or by uptake as a fluid inclusion [32].

1.4.1 Sources and transport of organic matter

The organic matter present in the depths of caves may have very different origins: it may come from the overlying environment in the form of aerosol particles, organic compounds transported by water or fauna (allochthonous production), or it may be produced by microorganisms living inside the cave (autochthonous production). Organic matter is composed of several fractions, so the transport includes dissolved or colloidal particles as well as particulate components. While the hydrophilic fraction of organic matter is easily leachable, the hydrophobic component is only leachable when the water causes the colloid materials to detach and transport. Once percolation water reaches the zone where rainfall saturates the deeper part of the soil (known as "vadose zone"), part of the dissolved organic matter is almost instantly adsorbed onto the surface of the calcium carbonate crystals and therefore sequestrated from microbial activities [27]. However, the high concentration of CO_2 in the vadose zone is indicative of root respiration, biodegradation and other biological activities. In fact, microorganisms living in this zone use organic matter as a source of energy.

At this point, some questions arise spontaneously: what kind of organic matter reaches the deepest part of the caves? And in what amount? The answers to these questions are related to the chemical and physical properties of the organic matter transported. In fact, the hydrophilic components are easily leachable but they are the most highly biodegradable. On the other hand, hydrophobic molecules are less leachable but more persistent since they are not readily available for microbial activity.

The transport is a crucial feature for the study of organic matter in the speleothems. As already stated, various fractions have different types of transport. Transport is influenced by several factors, both biotic and abiotic. For instance, rate and duration of infiltration depend on bedrock typology and type of flow path. These key parameters are essential not only to estimate the duration of transport and the degree of contact between mineral surfaces and water, but also to assess the nature of organic matter stored in the speleothems. As an example, caves characterized by rapid infiltration present a higher amount of organic matter compared to those with a slow infiltration rate [27]. The "soil leaching" is the main means of transport of organic matter formed on the surface and carried deep down by percolating water. Soil type, solid and solution phases and microbial activity are the main abiotic and biotic factors that influence this process. Soil may, in turn, be disrupted by natural events (such as fires or floods) or human activity: a change in soil type may, consequently, affect the transport of organic matter. Attention must also be paid to the time lag between the organic matter present on the surface and that incorporated in stalagmites and flowstones due to the slow turnover of organic matter in the soil. The variability of the temporal lag depends on type of transport, thickness of the soil and type of organic matter carried. Clearly, the response of the climatic signal is strongly dependent on the type of organic material present in speleothems, so further research on this issue is needed [32].

1.4.2 Flood events and mud layers

The ability of speleothems to reveal information about specific events has been further investigated. Stalagmites and flowstones consist of calcium carbonate in the form of calcite or aragonite. However, during flooding events, inclusions of clayey sediments can occur providing crucial information on the frequency of flooding and on isolated extreme flood events [33]. As for organic matter, sediments are distinguished by their allochthonous or autochthonous origin: the former are transported from outside while the latter are formed inside the cave due

to breakdown or weathering of the bedrock. The allochthonous detritus found in speleothems have very different origins including bird guano, soil particles, aerosols, soot, silt, clay and mineral grains of iron oxyhydroxide [34].

The size of the cave entrance acts as the first barrier. When the sediments enter the cave, a gravitational gradation occurs: coarse and heavy sediments are transported to the bottom of the flow while the fine particles are suspended towards the surface. This gradation is also found in the sedimentary sequence, which is formed when the water flow has a reduced energy to transport the particles. Some caves have ceilings coated with clay sediments, which means that the cave was once completely flooded and totally filled with clay.

Another proof of extreme flooding is the presence of thin layers of fine-grained clay and silt, deposited by muddy water (slackwater facies) in parts of the cave not easily reachable by the water flow. During flooding the cave is filled with muddy water that can reach the ceiling. When the flow is reduced, part of the water remains in the cave forming subterranean lakes where clay and silt are deposited. These silty and clayey layers are cemented by calcite crystals precipitated as a result of oversaturation of calcium carbonate due to the degassing of CO_2. Stagnant water eventually disappears due to evaporation or infiltration of the water at greater depths. The layers of aragonite formed on the loamy-clay layers are coated with a film of water that allows the speleothems to continue growing by precipitation of calcium carbonate [33].

Caves are very stable environments, where erosion and distortion rarely occur. This makes speleothems excellent archives: they can be precisely dated and provide excellent proxies for specific floods. Beyond recording isolated events, speleothems are able to preserve other environmental proxies with the same time scale. Thus it is possible to reconstruct not only the single extreme flood event, but also the environmental drivers that may have generated it. Among these, the land use change is of considerable importance since it can alter both the intensity and the rate of water infiltration and the amount of debris and organic matter reaching the cave [34].

1.4.3 State of the art

Fluorescence techniques have been widely used to detect the origin and characteristics of organic matter in speleothems. Some research studies suggest that the preferential process of inclusion of organic matter is adsorption onto the surfaces of carbonate crystals, followed by uptake. The type of organic material is characteristic of a single event: this makes organic matter a valuable tool to trace back specific phenomena. Furthermore, the structure of the organic matter found in speleothems is similar to fulvic acids, although it is more complex. Some studies show that there is a direct correlation between the degree of complexity of the molecule and the extent of its adsorption on crystalline surfaces. In addition, lipid biomarkers preserved in organic matter can provide information on land use in the surroundings of the cave but no precise temporal details have yet been achieved. There are still many open questions about how transport, residence time and percolation rate can alter organic material. Further research is needed to understand how organic matter is preserved in speleothems and which are the most robust proxies for reliable paleoclimatic reconstructions [36, 33, 28].

Speleothems are very suitable for isotopic dating, especially for the uranium-thorium series. As already mentioned, thorium originates exclusively from uranium decay, since speleothems grow in a stable environment where external contamination of this element can be excluded. Moreover, stalagmites and flowstones preserve many useful proxies for paleoclimatic reconstructions. The analysis of the $^{18}O/^{16}O$ ratio preserved in $CaCO_3$ reveals the percolation water temperatures recorded throughout the entire duration of speleothem growth. Also, the isotopic composition of the carbon atoms of calcite detects changes in vegetation, soil and humidity conditions in the ecosystem above the cave. The combination of carbon and oxygen isotope analysis enables the reconstruction of past flood events and variations in summer monsoon intensity. According to recent studies, the thickness of the bands and the growth rate of speleothems may depend on climatic conditions. However, the relationship between climate and growth of stalagmites is very complex and not yet completely clear as it involves many variables [36].

At present, paleoclimate reconstructions are widely based on the analysis of biomarkers. These molecules are very resistant to biodegradation and hold crucial information. As mentioned above, *n*-alkanes are excellent biomarkers because they are able to detect changes in vegetation cover related to climate change. They are in fact components of the cuticular waxes of plants that provide information about the hydrological and climatic conditions of the past. These molecules have been used in this research work precisely because they are persistent and well preserved in speleothems [30, 33].

Moreover, fluorescence analysis of stalagmites has identified the presence of PAHs, which are valid indicators of past combustion processes. There are still many unanswered questions about how to discern their anthropogenic or natural origin and how transport (adsorption on the surface of particles or in solution) can affect concentration and amount of PAHs found in speleothems. Furthermore, a research study analyzed a cave characterized by a thin and sloping overlying soil. During heavy monsoonal rains, water erodes very quickly the soil and carries organic material deep into the cave. When a fire occurs on the overlying ground, water in contact with soil increases its concentration of PAHs for a short period of time and when it percolates, it enriches the stalagmites with these organic proxies. Monitoring the concentrations of PAHs helps to identify individual fire events [28, 38, 39]. Nonetheless, this field of research is right at the beginning. A study shows that the amount of PAHs found in speleothems is comparable to the amount in soil samples above the cave [37]. PAHs are not very soluble in water, so they are present at low concentrations; however, these results show that PAHs are present in speleothems in measurable concentrations. It is not yet completely clear how the deposition of these organic molecules occurs because the mechanisms that influence it are highly site-specific and depend on the size and depth of the cave, the thickness and type of soil, surface vegetation and frequency and extent of fires. The analysis of speleothem PAH distribution in this research shows that about 90% of them are low-molecular-weight molecules. These data differ significantly from the above soil samples because many factors influence the amount and type of PAHs found in stalagmites. This is the only study of the

kind so far, and the authors point out that their analyses are only explorative due to method issues and because the cave is very deep. Therefore, the transport from the surface is very long so the molecules found in the stalagmites are not very representative [37]. The lack of other studies conducted on these organic molecules preserved in stalagmites makes the current research work very innovative despite the many difficulties related to resolution, low concentrations and contamination risk. The transport from the surface to the depth of the cave is a very complex and still little known mechanism that affects several variables so caution must be taken when analyzing the proxies found in speleothems. Some researchers suggest broadening the analysis of stalagmites and flowstones on different karst soils and to track multiple soluble organic molecules to better understand how the transport occurs and what are the most influential variables. Moreover, a better extraction would allow a more accurate study of the deposition and distribution of PAH compounds in speleothems [37].

Speleothems were chosen among several environmental archives for their ability to simultaneously record discrete past events and multiple environmental proxies. The aim of this research is to use these particular features of speleothems to reconstruct single fire events, in terms of frequency and intensity. Currently, only a small part of the information stored in the speleothems is known. Investigations concerning the presence of fire biomarkers and the possible data provided by them are still at an early stage. Hence, this thesis is an innovative tool for the analysis of speleothems using an organic multi-proxy approach.

1.5 THE KNI-51 CAVE

1.5.1 Climatic conditions and geographical location

The highest temperatures on the Australian continent are in the north, closer to the equator. Here the climate is tropical, with alternating dry and wet seasons, in response to the oscillation of the tropical rain belt (north or south of the equator). High summer temperatures generate a low-pressure zone in the mainland that draws ocean monsoonal winds from December to April. As a result, summers are hot and wet while winters are cold and dry. The rainfall pattern is irregular and varies every year [39].

Figure 1.8. Geographical location of KNI-51 cave and the Kimberley region [40].

The KNI-51 cave is located in the Kimberley region of northwest Australia (15° 18' S, 128° 37' E, 100 m altitude). This territory is characterized by mean annual temperature ranges from a minimum of 20.7 °C to a maximum of 35.1 °C. In terms of annual precipitation, it is between a minimum of 424 mm and a maximum of 838 mm; the highest precipitation is 1564 mm per year. Rainfall is not evenly distributed throughout the year: 90% is concentrated in the months between November and March. Periods of aridity are reoccurring about every ten years, while the more severe drought events are usually concomitant with El Niño (ENSO) events. This part of Australia is affected by several meteorological phenomena. Tropical Cyclones (TC) and the Indonesian-Australian summer monsoon (IASM) are the main causes of heavy rainfall, especially during summer [34, 35].

Tropical cyclones are low-pressure systems that form in the tropics, where sea surface waters rise above 26.5 °C. Their irregular trend determines a rather long and variable duration: from several days to weeks.

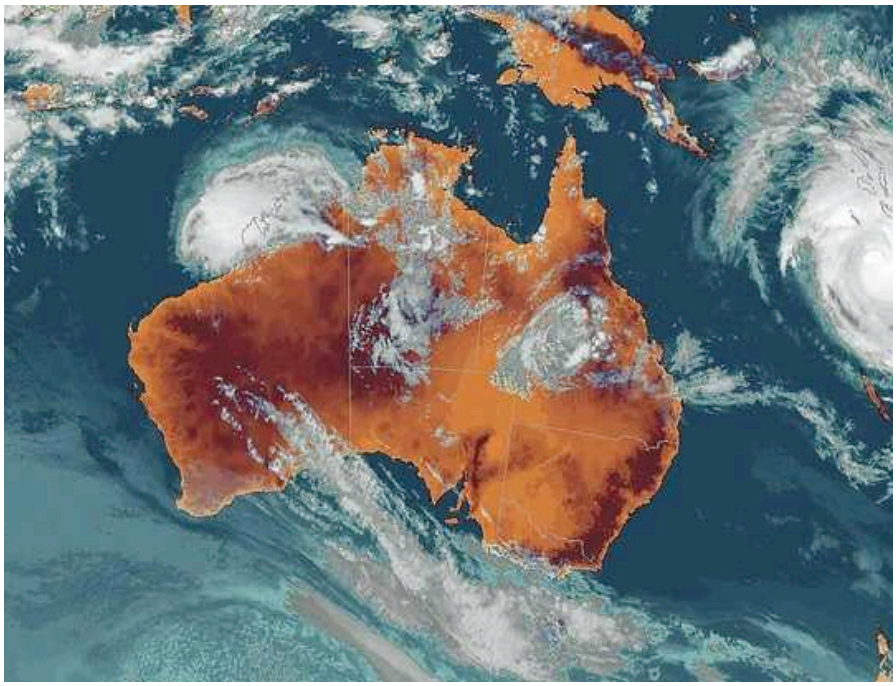

Figure 1.9. A tropical cyclone hitting Northern Australia [43].

Their characteristic shape consists in a body of spiraling thunderstorms rotating around a fulcrum (eye of the cyclone) where winds are the strongest and rains never stop.

Cyclones dissipate when they hit land destroying their structure or when they move to cooler surface waters [43].

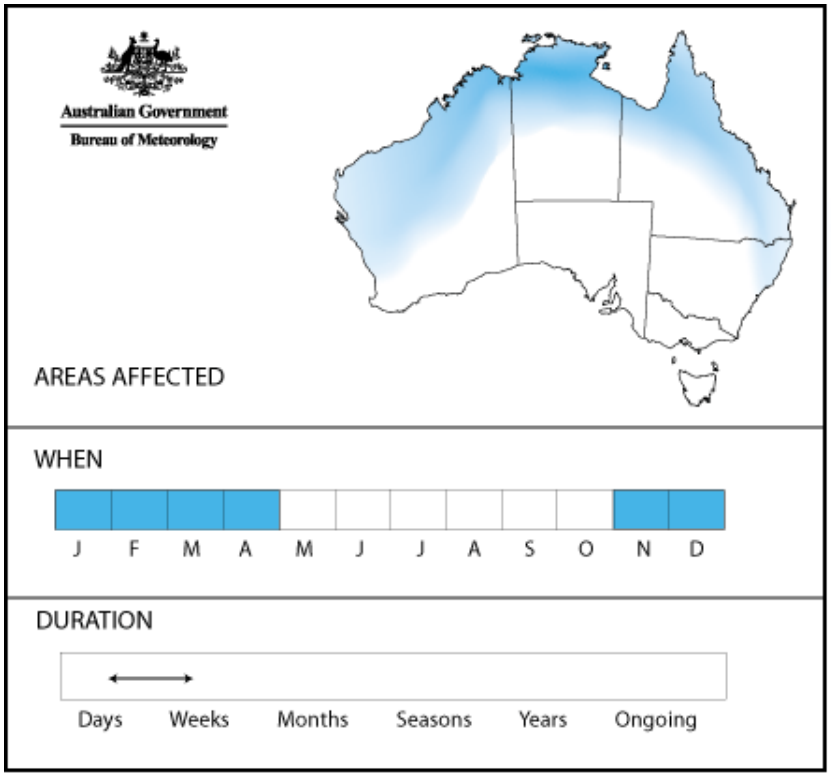

Figure 1.10. Occurrence, duration and areas affected by tropical cyclones [43].

These phenomena are responsible of extreme rainfall events and their activity is not clearly connected to ENSO. Some studies describe a possible past relationship between these two phenomena, followed by a gradual decoupling over time [34, 35].

Another characteristic climatic feature of this area is the north-western Indonesian-Australian summer monsoon (IASM), which usually starts in mid-end of December, during the Australian summer [34, 35]. The monsoon is a seasonal wind that causes heavy rain over a vast region. The name "monsoon", in fact, finds its origin in an Arabic word meaning "season". In Northern Australia, the monsoonal period lasts from October to April, but can be shorter, starting later and ending earlier. The beginning of the monsoon coincides with the reversal of the winds, which usually occurs towards the end of December, near Darwin [44].

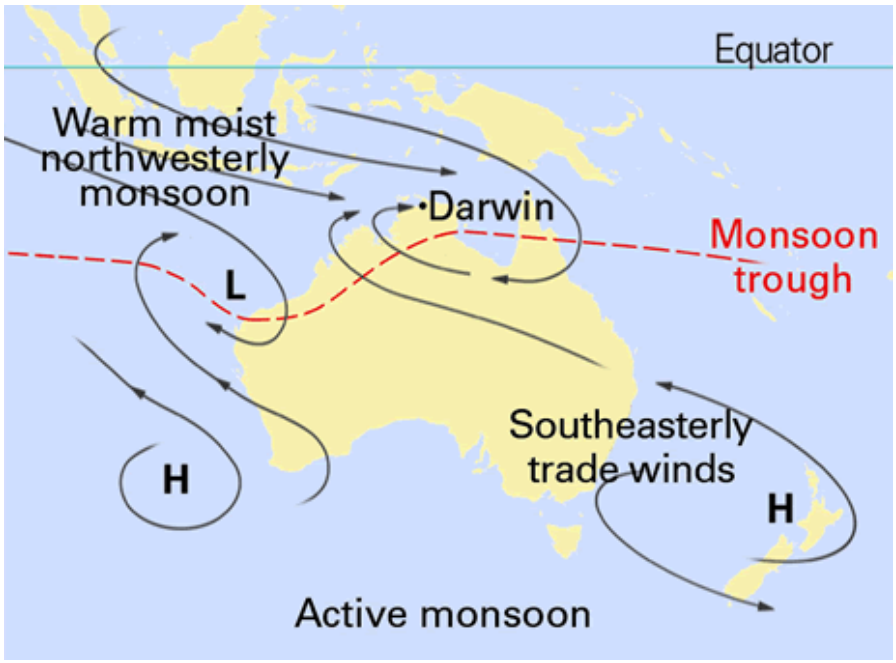

Figure 1.11. The active phase of the north Australian monsoon. The dashed red lines show the oscillating position of the monsoon trough: it shifts north or south from the equator [45].

The monsoon forms because the mainland heats up faster than the ocean (water has greater thermal inertia) and causes a difference in pressure with the consequent formation of a large sea breeze. This wind blows from the ocean to the mainland where moisture accumulates, generating the monsoon trough: a center of intense precipitation and cloudiness. When the monsoon moves over a region it will affect its meteorological conditions and this area will therefore be affected by monsoonal rainfall. The monsoon period may be followed by a period of "pause"

which is characterized by isolated thunderstorms and rainstorms. In the north of Australia there are about three monsoons active during the wet season (from the end of December to mid-April). The “monsoon retreat” is the end of the last monsoon of the year [44]. The intensity of the Indonesian-Australian summer monsoon (IASM) is influenced by the Madden-Julian (MJO) oscillation events that contribute to the distribution of the summer precipitations. There are also cold surges originating on the Siberian plateau that may trigger a deep convention zone in Australia, activating the IASM.

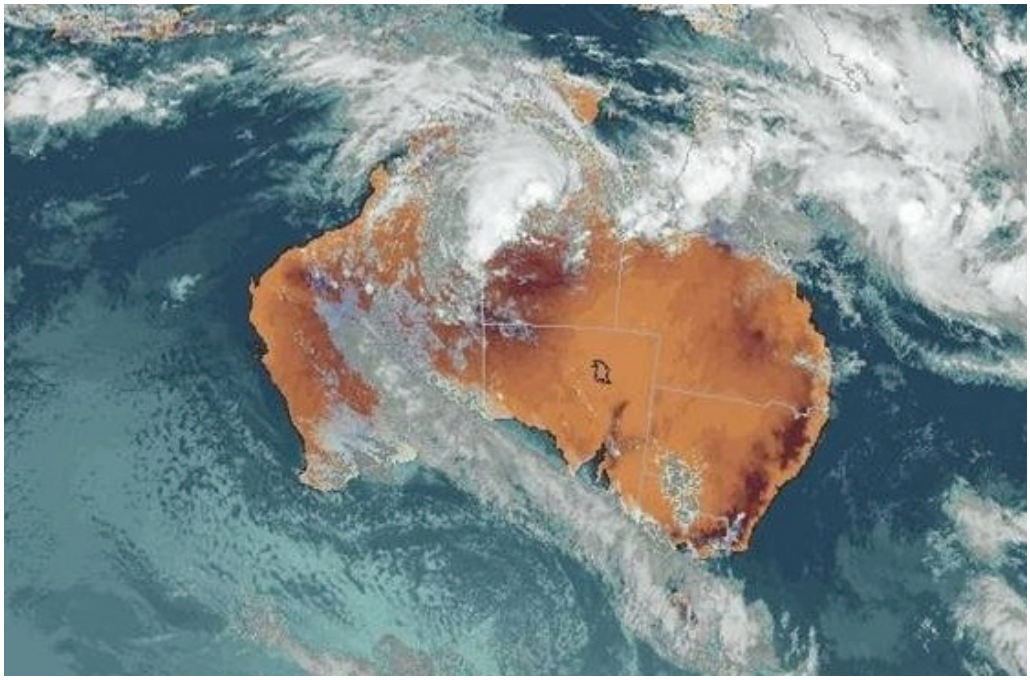

Figure 1.12. A satellite image of an active phase of the Madden-Julian Oscillation event [34].

The most influential climatic factor of the Australian continent is certainly ENSO. ENSO stands for El Niño-Southern Oscillation: it is a natural phenomenon consisting in the oscillation between periods of prolonged heating (El Niño) and long periods of cold temperatures (La Niña). This natural cycle, whose duration varies approximately from one to eight years, affects the central and eastern tropical Pacific areas.

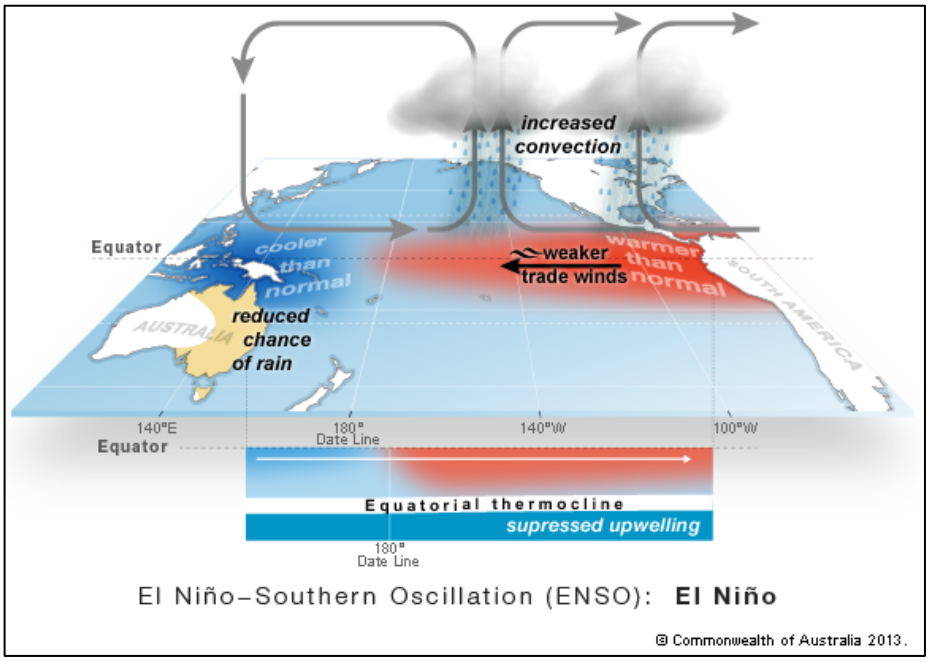

Figure 1.13. El Niño phenomenon [46].

During the El Niño phase, the sea surface temperature exceeds average values. This causes a shift in atmospheric circulation that weakens or even reverses the trade winds. Areas affected by these weather conditions present high cloud cover and heavy rainfall. Precipitation initially develops in Northern Australia and then spreads to central and eastern parts of the continent [45].

On the other hand, La Niña begins when temperatures in the Eastern Pacific Ocean cool down while those in the Western Pacific Ocean warm up. The temperature gradient strengthens the equatorial trade winds, thus triggering the cold oscillation of ENSO. These strong winds alter surface currents by pushing deep, cold waters towards the surface, further cooling the tropical and eastern

Pacific Ocean. Trade winds also shift the warm surface waters westward: they accumulate in the western Pacific and Northern Australia, where temperatures rise as cloud cover and precipitation increases.

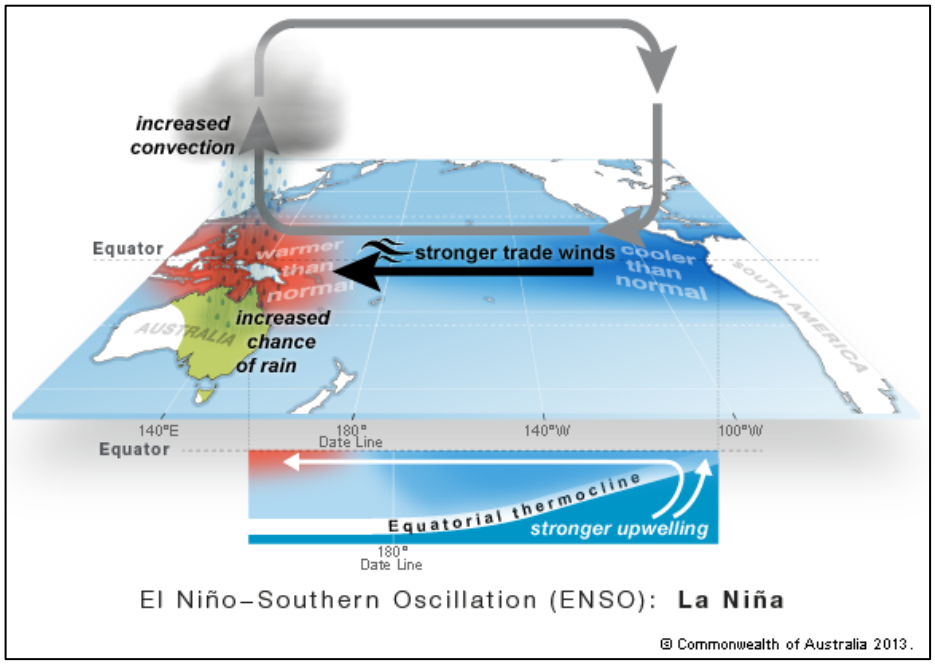

Figure 1.14. La Niña phenomenon [46].

The situation is diametrically opposed in the Eastern and Central Tropical Pacific where cold waters emerged on the surface reducing the probability of precipitation. Although each event in La Niña has specific features, it generally leads to an increase in precipitation throughout the Australian continent. More precisely, in the north of Australia, it can cause the formation of more tropical cyclones and the beginning of a new monsoonal phase [46].

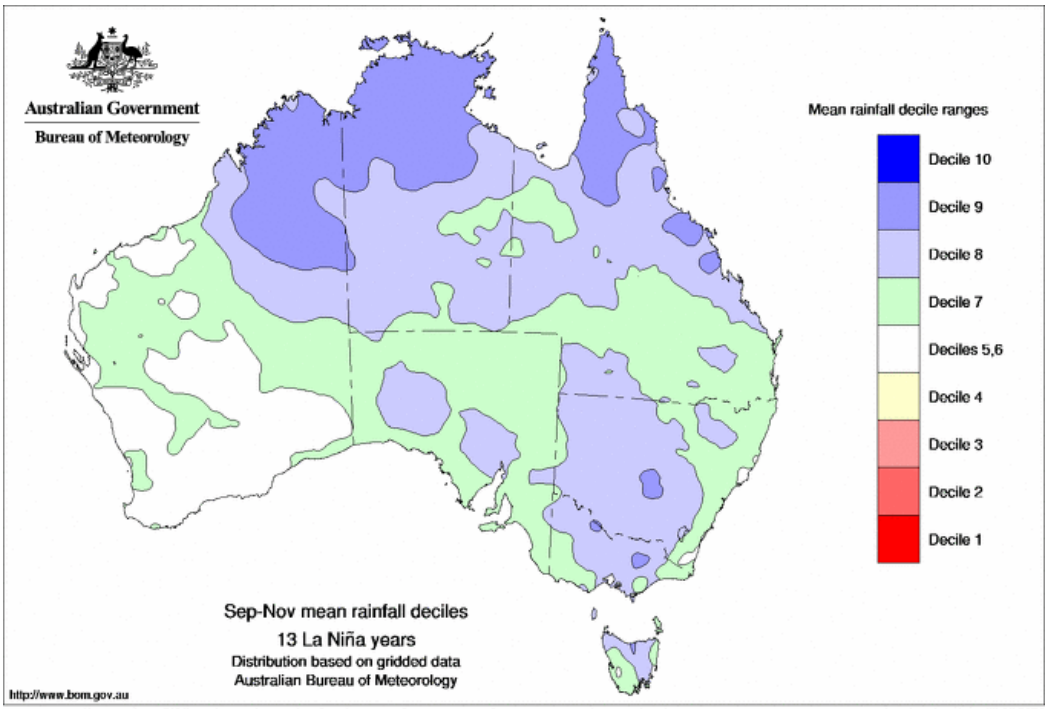

Figure 1.15. Spring precipitation during La Niña events [48].

El Niño weakly influences the eastern Kimberley region. Extreme drought events usually coincide with intense El Niño events, but precipitation is not related to this phenomenon. On the contrary, the presence of La Niña may intensify rainfall during spring and summer. However, certain studies report that it is very likely that the relationship between precipitation and ENSO has changed over time. It is therefore reasonable to suppose that a more intense correlation between ENSO and IASM may have existed in the past [41].

1.5.2 Features of the cave

The KNI-51 cave is of karstic origin and it is composed of Devonian limestone. Its dimensions are modest: it is 600 m long and it has a maximum depth of 15 m. Its morphology is similar to the several caves scattered in the surroundings: it has only one small entrance and almost horizontal paths. The vegetation above the cave is mainly Eucalyptus savannah growing on a thin soil that lies on limestone bedrock. The interior of the cave presents an almost stable temperature of about 28 °C and high humidity. As mentioned above, the rate of infiltration is a key parameter to understand the processes occurring within the cave. In this specific case, the estimated percolation time of the water to reach the cave is less than two months [41]. So, why was the KNI-51 cave chosen as an ideal site to reconstruct fire history?

The answer lies in the almost exclusive features of the speleothems growing in this cave. These stalagmites, mainly consisting of aragonite, have a very rapid growth rate of about 1-2 mm per year. Moreover, they contain abundant quantities of Uranium (between 5 and 15 mg/g) enabling them to be dated accurately. The combination of these properties guarantees a high-resolution reconstruction of past conditions [34].

1.5.3 KNI-51-11 stalagmite

Stalagmites extracted from cave KNI-51 were already broken at the time of collection; most are primarily composed of aragonite, a few of calcite [42]. They have been dated according to the uranium-thorium method at the University of the New Mexico Radiogenic Isotope Laboratory. The calibration of this dating procedure was then performed to increase the resolution of the stalagmite growth model. Mud layers were initially excluded from the model and subsequently dated through polynomials fit. Stable isotope analyses were performed in the same laboratory. These allow the reconstruction of the paleo-monsoonal activity with a nearly annual resolution [34, 39].

The aragonite stalagmite KNI-51-11 is the focus of this research. As already mentioned, aragonite is one of the three crystals forms of calcium carbonate (together with calcite and dolomite). The uranium content of aragonite minerals is usually higher compared to calcite and this increases dating resolution. The vertical sections, resulting from the cut of the stalagmite along the growth axis, present calcite incrustations. Brown lines due to muddy intrusions are also clearly visible. Mud layers are evidence of frequent flooding. In fact, during these events caused by at least three days of heavy rain, the cave floods: stalagmites are coated with mud and stop growing. The precipitation of calcium carbonate restarts only when evaporation or infiltration into the underlying layers reduces the presence of water. When stalagmites start growing again, they include mud particles within their stratified structure forming the brownish lines visible in the vertical sections [34, 39].

1.6 SOCIETAL AND CLIMATE CHANGE IN AUSTRALIA SINCE THE EUROPEAN COLONIZATION

The European arrival had a strong impact on the Australian environment, particularly in terms of wildfires. The Aborigines knew very well how to build and manage fires. Fires were part of their culture and a vital tool to survive in a very hostile environment. They developed an accurate method of burning the land so to reduce the impact and the extent of wildfires caused by lightning. In fact, a land that is regularly burned has less grass or wood that is, in turn, potential fuel. As a result, the next bushfire will probably have a less severe extension. The European settlement in Australia began in 1788. At that time, the continent was populated by 700,000 Aboriginal people, but Australia was still called “Terra Nullius”, no man's land. For this reason, settlers felt empowered to expel Aborigines, take possession of their land and declare it their property [34, 35].

Climate and environment have changed more rapidly with European colonization. Europeans needed precious natural resources to increase their incomes in global trade. They introduced new agricultural schemes, new biota, they promoted new forms of settlements and they chased away the Aborigines. Europeans were not very familiar with Australia's climate and territory, so various environmental problems arose.

When it comes to fire management, Europeans have had a very different approach from the Aborigines, which has led to a change in fire regimes and a reduction in fire-adaptive species. The absence of regular fire events has favored a natural ecological succession from grassy plains to forests, which has caused an increasing accumulation of fuel for potential extreme fires. The change in fire regime has had a huge impact on the surrounding biomass. In fact, it has caused a shift in vegetation structure that has affected the boundaries between savannah and forest. The difference in fire management between Aborigines and Europeans has been huge. The former often used small-scale fires, while the latter used mainly sporadic but more intense fires to expand agricultural activities. The European approach to fires is reflected in the change in the structure and composition of vegetation (the decline of savannah trees is one example) [36, 37].

Since the arrival of the Europeans, environmental change has speeded up at a remarkable pace. Today, forest fires are very frequent and widespread: they endanger many species and pose a serious threat to humans [34, 35].

Figure 1.16. An Australian extreme bushfire [51].

2. MATERIALS AND METHODS

2.1 REAGENTS AND STANDARDS

Pesticide grade solvents (SpS) include *n*-hexane, dichloromethane, acetone, methanol and 2,2,4, trimethylpentane, dichloromethane UpS and SpA Hydrochloric acid 34-37% produced by Romil Ltd. (Cambridge, UK) were employed in decontamination phases and as reagents. Anhydrous ACS Na_2SO_4 (≥ 99%) from Sigma Aldrich (Saint Louis, USA) was used.

Internal standard solutions with isotope-labelled molecules such as $^{13}C_6$-acenaphtylene, $^{13}C_6$-phenanthrene, $^{13}C_4$-benzo(a)pyrene acquired from Cambridge Isotope Laboratories and hexatriacontane from Sigma Aldrich were employed.

A solution of $^{13}C_6$-chrysene from Cambridge isotope laboratories was used as a recovery standard.

The PAH Mix-9 solution consisting of native compounds obtained by Dr. Ehrenstorfer (Augsburg, DE) and a *n*-alkanes C_{10}-C_{35} solution produced by Sigma Aldrich were employed.

2.2 INSTRUMENTAL EQUIPMENT

2.2.1 Clean room

The preparation of samples was carried out entirely in a class 10,000 organic cleanroom laboratory (ISO 7, < 10,000 particles/m^3) equipped with fume hoods, with the only exception of sub-sampling (the initial phase of the procedure). The clean room is located in the Department of Environmental Sciences, Informatics and Statistics at Ca' Foscari University.

This laboratory is very particular because the conditions of temperature and pressure are constantly monitored to ensure their stability. The clean room consists entirely of stainless steel to minimize organic contamination. Moreover, an effective filter system prevents the introduction and accumulation of atmospheric aerosols. In the laboratory, air circulation forms a laminar flow from

the ceiling down to the floor. This system prevents the formation of airflows or vortexes that could contaminate the samples.

Anyone entering the clean room must wear full lab coat and shoes used exclusively in this laboratory. These are some of the indications of the cleaning protocols that help to preserve minimal contamination conditions inside the clean room.

2.2.2 Turbovap II

The analytes extracted from the samples were reduced in volume using Turbovap II (Caliper Life Science, Hopkinton, CA, USA). The operation involves a maximum of six samples, which are transferred into glass tubes and then placed in a thermostatic bath at constant temperature and pressure. This is connected to a nitrogen source: the gas streams through the glass tubes forming a helical flow that generates a vortex. As a result, the evaporation of the solvent is more homogeneous. The instrument is also equipped with optical sensors that stop the concentration once the volume of 500 μL is reached.

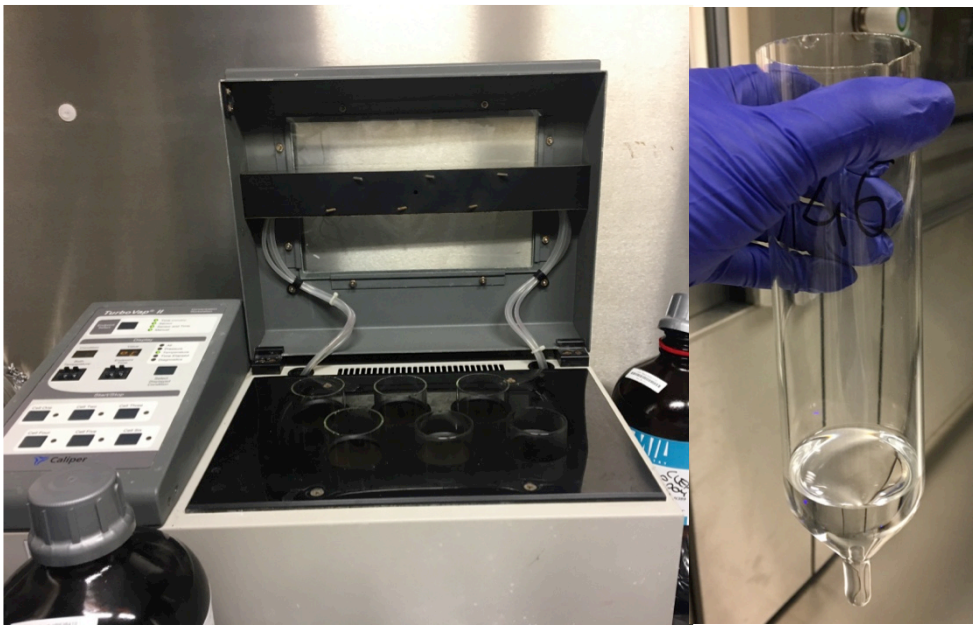

Figure 2.1. Left: Turbovap II. Right: glass tube containing the sample placed inside the instrument.

2.2.3 Gas Chromatography – Mass Spectrometry (GC-MC and GC-MS/MS)

Gas chromatography coupled to single quadrupole mass spectrometry was used for *n*-alkane analysis, while gas chromatography coupled to triple quadrupole mass spectrometry was applied for PAH analysis.

n-alkanes analysis requires the use of an Agilent Technologies 7890A GC system coupled with an Agilent Technologies 5975C single quadrupole mass spectrometer. For PAHs, a Thermo Scientific TRACE 1310 gas chromatograph coupled with a TSQ 9000 triple quadrupole mass spectrometer was used.

By combining gas chromatography and spectrometry, it is possible to identify molecules with low detection limits and achieve good quantitative results. The molecules are first volatized in the GC injector and then pushed into a capillary column coated with a stationary polymer phase. Here the temperature is programmed to increase gradually, according to a temperature program that includes ramps and static phases. Compounds enter the mass analyzer according to their retention times in the capillary column. Once inside, the electron impact source fragments the molecules.

Positive ions are pushed by electrostatic repulsion towards the quadrupole, which detects the ions and selects the characteristic mass-to-charge ratio in order to minimize interferences. The electron multiplier amplifies the signal and this is then processed in a chromatogram. Each peak in the graph identifies a specific compound. In fact, each molecule is characterized by a unique retention time and a specific m/z ratio visible in the peak.

The triple quadrupole mass spectrometer consists of two mass analyzers: the first quadrupole and the third quadrupole. They are separated by an additional quadrupole in total transmission filled with Argon (inert gas) to serve as collision cell.

The molecules, already fragmented during the passage into the first quadrupole, are reduced into even smaller parts before reaching the third quadrupole. The fragments thus formed enable a more precise identification of the compound due

to their greater specificity. This provides a better qualitative analysis and good quantitative results: the compound, has been identified twice, in the first and third quadrupole.

2.3 PREVENTING LABORATORY CONTAMINATION

PAHs and *n*-alkanes are present in stalagmites as trace compounds, so possible sources of sample contamination need to be considered to ensure accurate results. This must be done scrupulously at every stage of the analytical procedure. Sources of contamination are the most diverse: vials containing the samples, particulate matter in the laboratory air, reagents, equipment used and operators themselves.

Minimizing contamination is crucial because it can increase background noise or interfere with analytes causing signal distortion. The risk of contamination increases when the analyte concentration is low. In this case, the procedure requires extremely low concentrations of the analytes, so it is essential to pay the utmost attention to any source of contamination at every stage of sample preparation.

All equipment and glassware are first pre-washed with a Contrad® aqueous solution (5%). Glassware is heated in a muffle furnace for 4 hours at 400 °C. Decontamination of all tools is carried out first with *n*-hexane and then with dichloromethane: the operation is repeated three times. Furthermore, avoiding the use of plastic containers or instruments is an additional precaution to reduce the risk of contamination. Prior to subsampling, the fume hood is cleaned with solvent and fully coated with aluminium foil. The next phases of sample preparation are carried out in the clean room, following the cleaning protocols.

2.4 SAMPLE PREPARATION

2.4.1 Stalagmite preparation

KNI-51-11 stalagmite was sliced into vertical sections, parallel to the growth axis. The tool used in this operation is a water-cooled circular saw. It was then sent to the Radiogenic Isotope Laboratory at the University of New Mexico where it was dated using the uranium-thorium series method. Dating was followed by calibration of a high-resolution age model of the stalagmite. By combining this model with stable isotopic analysis carried out in the same laboratory, it was possible to reconstruct the paleo-monsoonal activity with a resolution of ~0.5-5 years [42].

Figure 2.2. Vertical section of the stalagmite KNI-51-11 analyzed in this research work.

2.4.2 Sample preparation

This section describes the analytical procedure developed at the Ca' Foscari University of Venice.

2.4.3 Sub-sampling (drilling)

The hand-held Dremel was used to produce 1g powder samples, for a total of 213 samples, which were analyzed by placing 1 blank for every 5 samples. The tips were immersed in a solution of *n*-hexane and dichloromethane and sonicate for 5 minutes. The surface of the stalagmite was first washed with *n*-hexane and dichloromethane and then drilled following the growth lines to obtain 1g samples corresponding to a perforation of a 1-2 mm layer. The powder was collected in 60 mL vials, closed by a cap with a perforable septum. The vials containing the samples were previously muffled and stored in clean room until the next steps.

Figure 2.3. Left: drilling the stalagmite. Right: vertical section of the stalagmite and measurement in mm.

2.5 EXTRACTION AND CONCENTRATION

Internal standards were added using an SGE™ eVol™ automatic portable analytical syringe by injecting 50µL of $^{13}C_6$-acenaphthylene, $^{13}C_6$-phenanthrene, $^{13}C_4$-benzo(a)pyrene (1 ng μL^{-1}) and 50µL of hexatriacontane (50 ng μL^{-1}) solution to each sample.

10 mL of UpS DCM were added using the graduated cylinder to prevent evaporation of volatile compounds. 2 mL of 34-37% HCl were injected with a disposable syringe through the septum of the vial to hold the volatile species derived from the dissolution of the aragonite matrix. Samples were soaked in ice to reduce the speed of the reaction. They were repeatedly mixed with vortex to facilitate the dissolution of the analytes and their transfer into the organic phase.

An additional 2 to 3 mL HCl were added if the matrix was not completely dissolved. When dissolution was complete, 10 mL of *n*-hexane were added and further vortex mixing was carried out, before letting the organic and inorganic phase separate completely. The extracts were transferred with a pasteur pipette into another vial. The organic phase was transferred with a pasteur pipette into another vial. The entire extraction procedure was repeated twice with 5 mL of DCM and 5 mL of *n*-hexane, collecting the extracts from the three extraction steps together. ~2 g of anhydrous Na_2SO_4, previously oven dried at 150 °C for 24 hours, washed with DCM and *n*-hexane in the sonic bath and stored in *n*-hexane before being used in the procedure, were then added to each sample. This compound has the function of anhydrifying the samples and buffering their pH.

2.5.1 Volume reduction

The Turbovap II has been set at 23 °C and used to reduce the volume of the extracts. When the volume dropped to ~0.5 mL, 100 µL of isooctane were added to each sample in order to better preserve them by reducing the chance of evaporation. Extracts were further concentrated to a volume of ~100 µL and 20 µL of a 100 pg μL^{-1} $^{13}C_6$-chrysene were spiked to be used as a recovery standard.

Then the samples were transferred with a Pasteur pipette into a GC vial and refrigerated until analysis.

2.6 GC-MS ANALYSIS

A Trace 1310 GC-TSQ 9000 GC-MS/MS (Thermo Scientific) was used for the analysis of PAHs while a 7890A GC system coupled to a 5975C single-quadrupole mass spectrometer (Agilent Technologies) was employed for *n*-alkanes. Both instruments were equipped with a HP-5ms capillary column (60 m, 0.25 mm i.d., 0.25 μm film thickness, Agilent Technologies) with a stationary phase consisting of (5%-phenyl)-methylpolysiloxane. GC separation was carried out following this procedure:

PAHs:

- Injection temperature: 300 °C
- Transfer-line temperature 300 °C
- Oven temperature program:
    1. 70 °C for 2 min
    2. 10 °C min^{-1} to 200 °C for 5 min
    3. 8 °C min^{-1} to 280 °C for 5 min
    4. 5 °C min^{-1} to 310 °C for 9 min
- Carrier-gas: Helium, with a rate of 1 mL min^{-1}
- PTV Injector:
    - Mode: splitless
    - Temperature program: from 70 °C to 320 °C at 14.5 °C s^{-1}

n-alkanes:

- Injection temperature: 300 °C
- Transfer-line temperature: 300 °C
- Oven-temperature program:
    1. 50 °C for 5 min

2. 18 °C min-1 to 315 °C for 13 min
3. Post-run of 315 °C for 15 min

- Carrier-gas: Helium, with a rate of 1.2 mL min^{-1}
- Injection mode: splitless (split valve open 1 min after the injection at 50 mL min^{-1})

PAHs were examined through the MRM (multiple reaction monitoring) mode so to achieve more accurate quantitative results of the analytes. This analysis was performed by tandem mass spectrometry using the triple quadrupole analyzer and by setting:

- first quadrupole in SIM mode
- collision cell to fragment the selected ion
- third quadrupole in SIM mode.

For the analysis of *n*-alkanes, the SIM mode of the single quadrupole mass spectrometer was selected: the electron impact source was set at 70eV and 230 °C and the initial temperature of the quadrupole at 150 °C. Agilent MSD Chemstation software was used to process the chromatograms generated by the instrument. Response factors were obtained by repeatedly injecting a solution of known concentration containing all native and labeled compounds. The quantification of analytes was achieved by the isotope-dilution method and corrected with the response factors.

The following pages sum up the mass-to-charge ratios (m/z) of molecular ions detected by GC-MS for both qualitative and quantitative analyses of PAHs.
As for *n*-alkanes, the analyses of all molecules (C_{11}-C_{36}) were performed in SIM mode by detecting molecular ions with a mass-to-charge ratio of 71, 99, 85 and 113. The mass-to-charge ratio of 71 was used for quantification.

Table 1. Mass-charge ratios of PAHs molecular ions for the qualitative and quantitative analysis

Quantitative Analysis						
Name	Retention time	m/z	Product Mass	Collision Energy	Quantifier ion	Qualifier ion
Naphthalene	11.55	128	77.7	20		x
Naphthalene	11.55	128	102	18	x	
Naphthalene	11.55	128	126.9	16		x
Acenaphthylene	15.34	151.9	101.9	26		x
Acenaphthylene	15.34	151.9	125.8	24	x	
Acenaphthylene	15.34	151.9	150	28		x
Acenaphthylene C13	15.34	158	156	28	x	
Acenaphthene	15.81	152.8	152.2	18		x
Acenaphthene	15.81	154.1	152.4	24		x
Acenaphthene	15.81	154.1	153.1	16	x	
Fluorene	17.25	165	163	30		x
Fluorene	17.25	166.1	115	38		x
Fluorene	17.25	166.1	165.1	16	x	
Phenanthrene	21	176	149.9	24		x
Phentanthrene	21	178	150.9	28	x	
Phenanthrene	21	178	151.6	22		x
Phenanthrene C13	21	184	157	28		x
Phenanthrene C13	21	184	158	22	x	
Anthracene	21.2	176	149.9	22		x
Anthracene	21.2	178	151	32	x	
Anthracene	21.2	178	151.7	20		x
Fluoranthene	26.2	202	152.1	30		x
Fluoranthene	26.2	202	200	32	x	
Fluoranthene	26.2	203.2	201.1	32		x
Pyrene	27.05	202.1	198.6	30		
Pyrene	27.05	202.1	200	10		
Pyrene	27.05	203.3	201	38		
Retene	28.4	234	202.9	36		x
Retene	28.4	234	219.1	36	x	
Benzo(a)anthracene	31.55	225.9	224.1	34		x
Benzo(a)anthracene	31.55	228	226	28	x	
Benzo(a)anthracene	31.55	229.2	227.1	30		x
Chrysene	31.7	225.9	200	28		x
Chrysene	31.7	225.9	223.9	32	x	
Chrysene	31.7	229.2	227.1	30		x
Chrysene C13	31.7	232	230	32	x	
Benzo(b)fluoranthene	36.5	126.1	113	12		x
Benzo(b)fluoranthene	36.5	250	248.3	34		x

Benzo(b)fluoranthene	36.5	252.1	250.1	32	x	
Benzo(k)fluoranthene	36.6	250	248	32		x
Benzo(k)fluoranthene	36.6	252.1	226.1	28		x
Benzo(k)fluoranthene	36.6	252.1	250	34	x	
Benzo(a)pyrene	38	250	248	36		x
Benzo(a)pyrene	38	252.1	250	34	x	
Benzo(a)pyrene	38	253.3	251.1	34		x
Benzo(a)pyrene C13	38	256	254	34	x	
Benzo(a)pyrene C13	38	257	255	34		x
Indeno(1,2,3-cd)pyrene	43.08	138.1	124.6	15		x
Indeno(1,2,3-cd)pyrene	43.08	274	272	35		x
Indeno(1,2,3-cd)pyrene	43.08	276.1	274	40	x	
Dibenzo(a,h)anthracene	43.22	276	274	38		x
Dibenzo(a,h)anthracene	43.22	276	275.1	26		x
Dibenzo(a,h)anthracene	43.22	278.1	276	34	x	
Benzo(g,h,i)perylene	44.28	137.7	136.8	16		x
Benzo(g,h,i)perylene	44.28	276.1	274.1	38	x	
Benzo(g,h,i)perylene	44.28	276.1	274.6	18		x

3. RESULTS AND DISCUSSION

3.1 AGE MODEL AND $\delta^{18}O$ RECORD

As the current work focuses on the reconstruction of fire history, isotopic dating and $\delta^{18}O$ record related to the KNI-51-11 stalagmite are crucial. These data, collected by Dr. Denniston's research team at University of the New Mexico Radiogenic Isotope Laboratory, are now displayed to provide a more accurate interpretation of the results obtained in this research work.

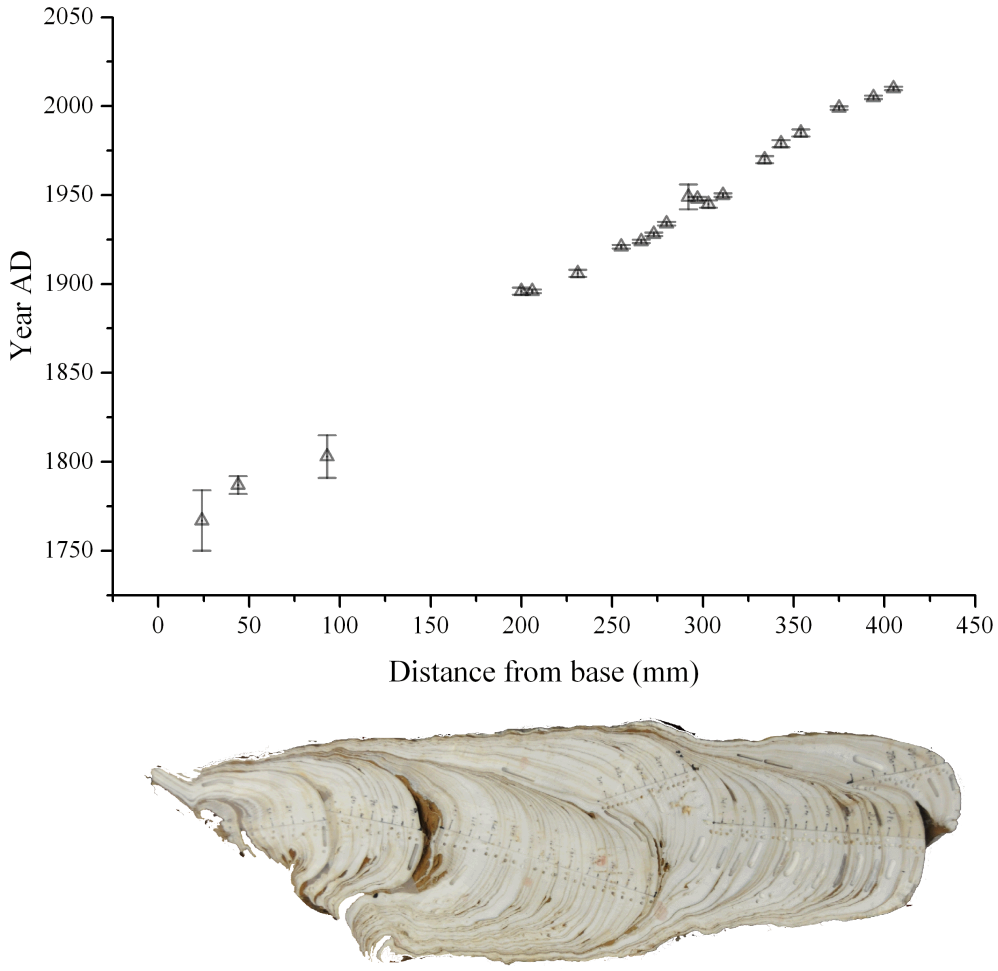

Figure 3.1. U/Th dates and age model for stalagmite KNI-51-11. Adapted from [42].

The stalagmite was dated using the high-precision uranium-thorium method [38].

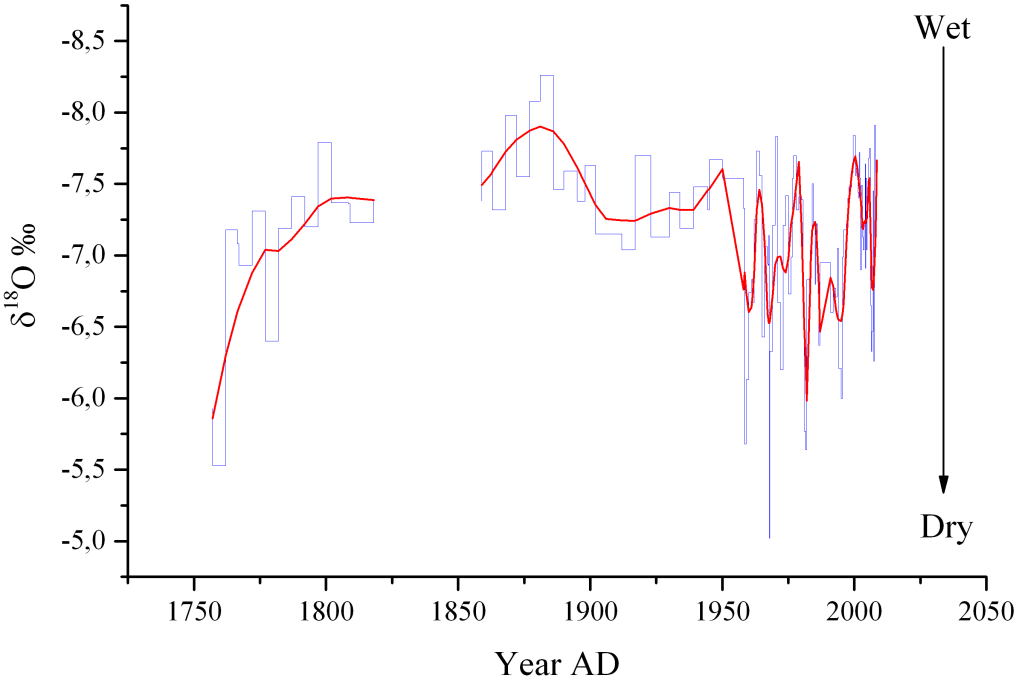

Figure 3.2. $\delta^{18}O$ record of the KNI-51-11 stalagmite (Smoothing: Lowess, 10 points). Adapted from [42].

Figure 3.2 shows the trend of $\delta^{18}O$. The $^{18}O/^{16}O$ ratio provides valuable information about past temperatures both at the surface and within the cave. As previously mentioned, speleothems form under conditions of isotopic equilibrium between percolating water and air inside the cave; hence, it is possible to reconstruct past temperatures for the entire growth period of the stalagmite. Furthermore, since $\delta^{18}O$ is an excellent tracer of monsoonal activity, its trend identifies dry and wet periods [2, 3]. In figure 3.2, low values (more negative) of $\delta^{18}O$ indicate wet periods while higher values correspond to dry ones.

3.2 POLYCYCLIC AROMATIC HYDROCARBONS (PAHs)

The analysis of polycyclic aromatic hydrocarbons (PAHs) as fire proxies is the core of this research work. PAHs are organic molecules composed of hydrogen and carbon atoms containing two or more aromatic rings; they are mainly formed during the incomplete combustion of organic matter, under oxygen deficiency. The main natural source of PAHs in the environment is biomass burning. Since every bushfire produces different combustion products, the analysis of PAHs is essential to collect information on the type of vegetation affected, fuel typology, temperature and humidity conditions [19]. PAHs are classified according to their molecular weight. Low-molecular-weight PAHs (LMW) are gaseous molecules containing one to three aromatic rings; medium-molecular-weight PAHs (MMW) have three to five aromatic rings, they are present both in vapor and particulate phases and they are not soluble in water; PAHs containing more than five aromatic rings are adsorbed on aerosol particles and they are hydrophobic. Molecular weight, not only determines the physical state or hydrophobicity of the molecules, but also affects their transport: LMWs are easily dispersed, while HMWs are adsorbed on airborne particles and then scavenged by precipitation [5, 6].

In the present research, eighteen PAHs stored in the stalagmite were analyzed. The following figures show the concentrations of the most significant individual PAHs in ng g^{-1} (powdered material) while the next two bar plots represent the number of samples (out of total) in which the compound is present and the average concentration of each PAH in the samples, respectively.

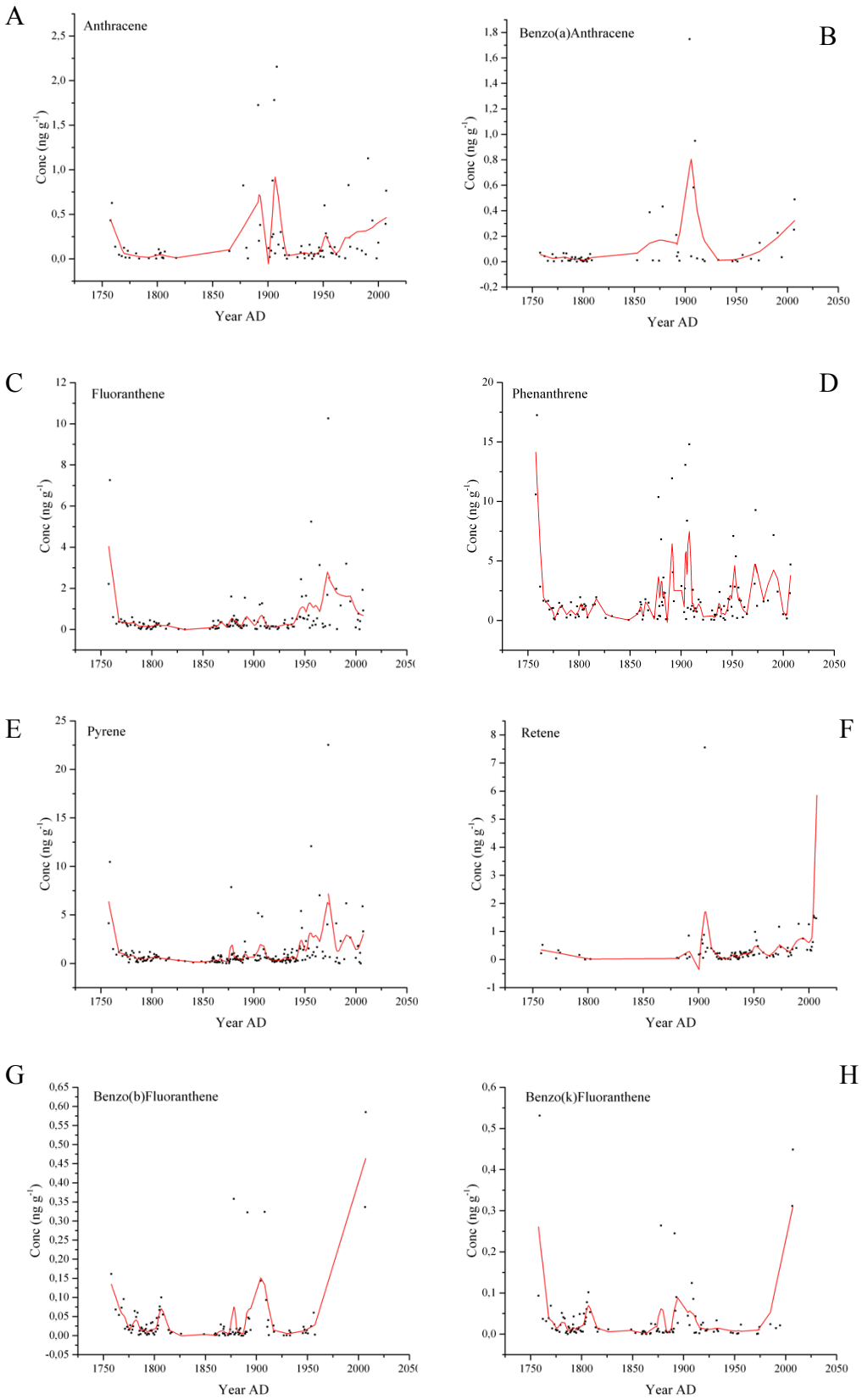

Figure 3.3. Concentration (ng g^{-1}) of the most significant PAHs found in the stalagmite KNI-51-11.

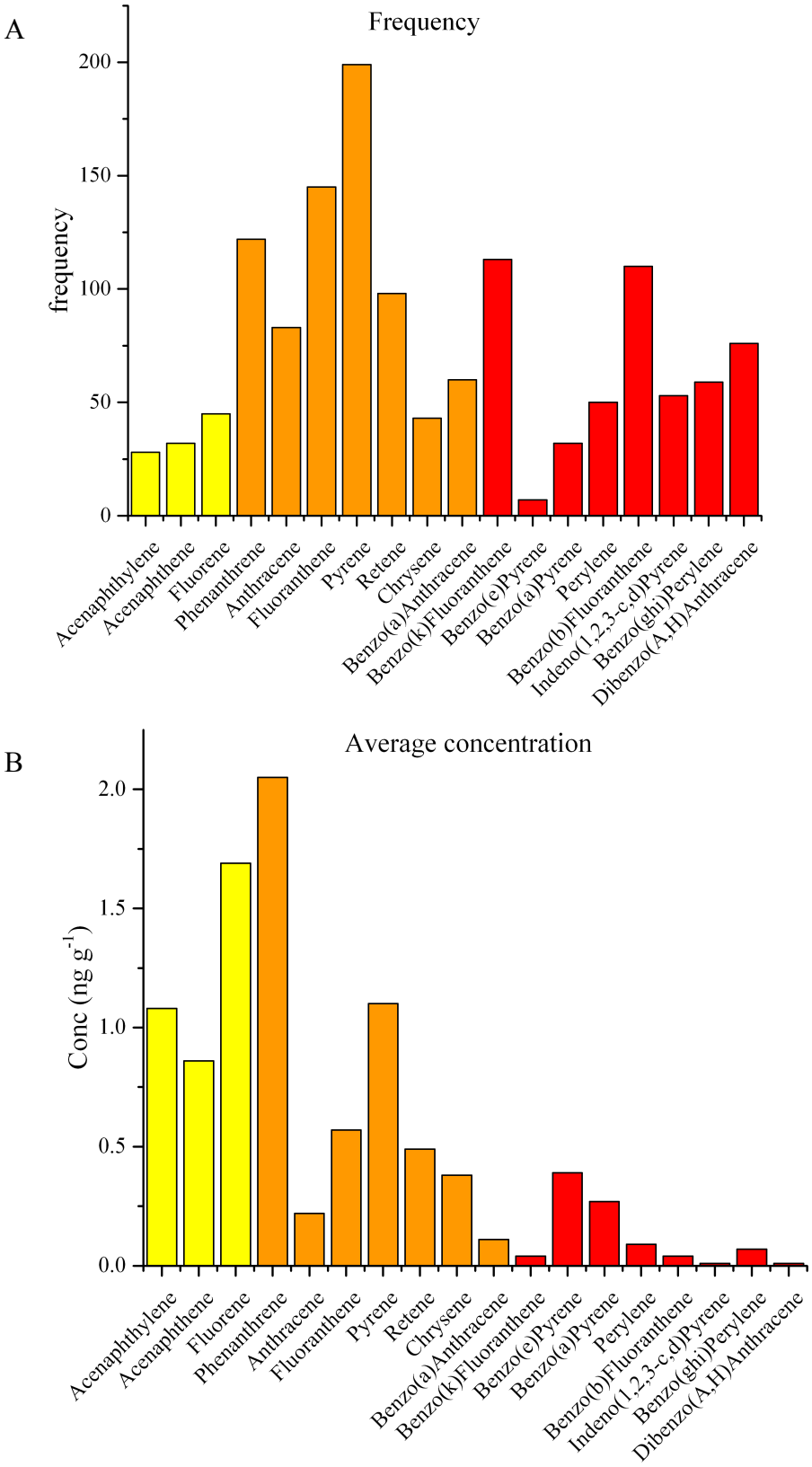

Figure 3.4.
A: number of samples in which the single PAH is present out of the total number of samples.
B: average concentration of each PAH.

The figures above show the trends of the most significant compounds meaning those present in the largest number of samples that do not necessarily have the highest concentrations (the other PAHs present very low concentrations, mostly below the detection limit). All trends show an initial decrease (more or less marked) and peaks around 1900, regardless of molecular weight (low, medium or heavy) and total concentration. The molecules with the greatest number of peaks are fluoranthene, phenanthrene, and pyrene while those with a strongly increasing trend at the end of the record are retene, benzo(b)fluoranthene, and benzo(k)fluoranthene.

As for histograms, the three colors represent the classes of PAHs based on molecular weight: yellow for light molecules (LMW PAHs), orange for medium PAHs (MMW PAHs), and red for heavy compounds (HMW PAHs).

Among the LMW PAHs (acenaphthene, acenaphthylene, and fluorene), fluorene is the predominant compound, with a maximum concentration of 11 ng g^{-1} and it is also the most present in the samples. As for the MMW PAHs, which consist of phenanthrene, anthracene, fluoranthene, pyrene, retene, chrysene, and benzo(a)anthracene, pyrene present the maximum concentration of 23 ng g^{-1} but the most significant compound in terms of frequency is phenanthrene.

In the HMW class of PAHs (benzo(k)fluoranthene, benzo(e)pyrene, benzo(a)pyrene, perylene, benzo(b)fluoranthene, indeno(1,2,3-c,d)pyrene, benzo(ghi)perylene, and dibenzo(a,h)anthracene) the most frequent compound is benzo(k)fluoranthene while perylene has the highest concentration of 3 ng g^{-1}.

Results show that medium-molecular-weight PAHs are the most present compounds in the samples and have the highest concentrations; in particular, phenanthrene is the most significant compound while pyrene is the most abundant PAH preserved in the stalagmite. LMW and MMW PAHs are always present in the samples whereas HMW PAHs usually have very low concentrations, often below the detection limit in several samples.

In the next page, fig. 3.5 displays the total concentration of LMW, MMW and HMW together with the total concentration of PAHs and $\delta^{18}O$ record of the stalagmite.

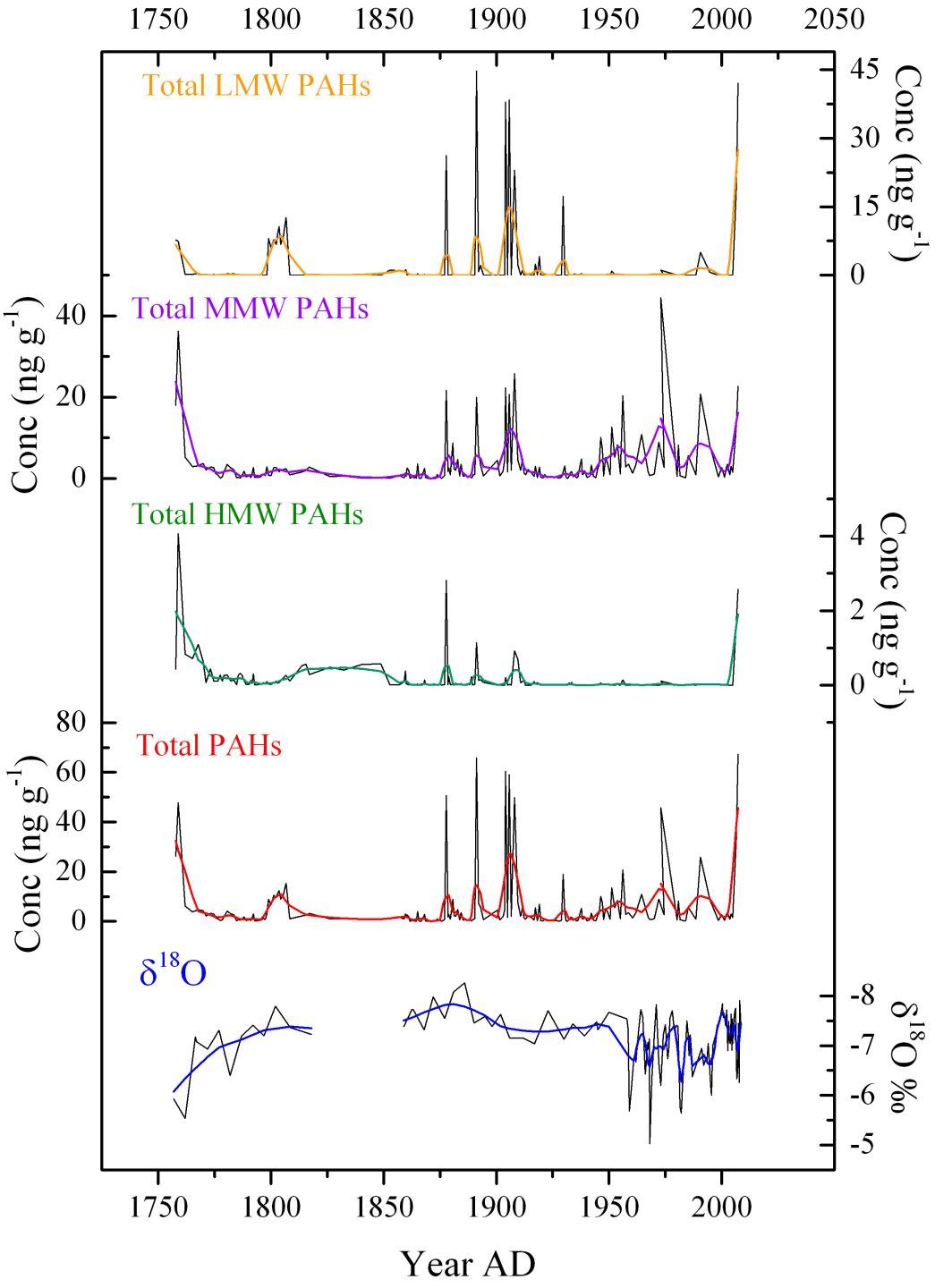

Figure 3.5. Top: concentration (ng g^{-1}) of Low, Medium and High molecular weight PAHs. Bottom: total amount of PAHs and $\delta^{18}O$ record of the stalagmite KNI-51-11.

The total concentration primarily results from the contribution of MMW PAHs, which are the most abundant compounds. The main source of these molecules is biomass burning, which occurs between 400-500 °C. More generally, the concentration of combustion products is related to the size of the single molecule: the larger the size, the higher the formation temperature, the lower its emission factor [52]. LWM and MMW PAHs are more abundant because their formation occurs at lower temperatures and corresponds to frequent low-medium intensity fires. In any case, the lower presence of LMW compared to MMW is due to the different chemical nature of these compounds that are more volatile, more soluble and more labile and therefore less easily preserved. High-molecular-weight compounds are scarce because their formation requires high temperatures, mostly associated with rare high-intensity fires or with the combustion of fossil fuels. The latter occurrence is unlikely because the KNI-51 cave is located in a remote area where the main anthropogenic activities are agriculture and pastoralism and the nearest town of Kununurra is 40 km away [41]. The absence of industrialized areas and the distance from towns and cities ensure that the site does not present any interferences of PAHs produced by industrial activities or traffic, so it is highly significant for tracing local-scale fire events.

Looking at fig. 3.5, all trends show a sharp initial decrease that probably indicates the final phase of an event that took place before the formation of the stalagmite and therefore it was not recorded in the archive. Furthermore, in this part of the graph, the relationship between $\delta^{18}O$ and the total amount of PAHs is evident: high $\delta^{18}O$ values correspond to high concentrations of PAHs and conversely. This means that between approximately 1750 and 1830, fire intensity was high during dry periods (higher values of $\delta^{18}O$) and low during wet periods (low values of $\delta^{18}O$).

Moreover, fig. 3.5 shows a clear change in fire activity since the late 1800s: the trend is very different from earlier periods because there is no link between $\delta^{18}O$ values (representing dry or wet conditions) and PAHs concentrations. The peaks indicate fire events of significantly greater intensity and frequency than in the past.

As it is evident from fig. 3.5, several peaks occur from the 1950s onwards, indicating a marked upswing in fire activity. As opposed to previous periods, the increase in fire intensity and frequency does not seem to be related to climate variations inferred by the $\delta^{18}O$ record, so these fires may be of a different nature from those occurring in the late 1700s and early 1800s. In addition, peaks are visible only in medium molecular weight compounds, (LWM and HMW display no remarkable peaks in this period), hence they indicate intense biomass burning that could be associated with other phenomena such as land use change. The record ends with a spike in total PAHs, resulting from contributions from all three classes of compounds.

3.3 *n*-ALKANES

n-Alkanes are valuable proxies for this research work because they reveal precious information about past vegetation and climatic conditions. These molecules, composed of hydrogen and carbon atoms, have only single bonds and are not soluble in water [20]. They are excellent biomarkers because their low reactivity and high resistance to biodegradation preserve them both during transport from the surface and after deposition in the stalagmite. The next graph (fig. 3.6) shows the trend of the total amount of *n*-alkanes during the three centuries of stalagmite growth.

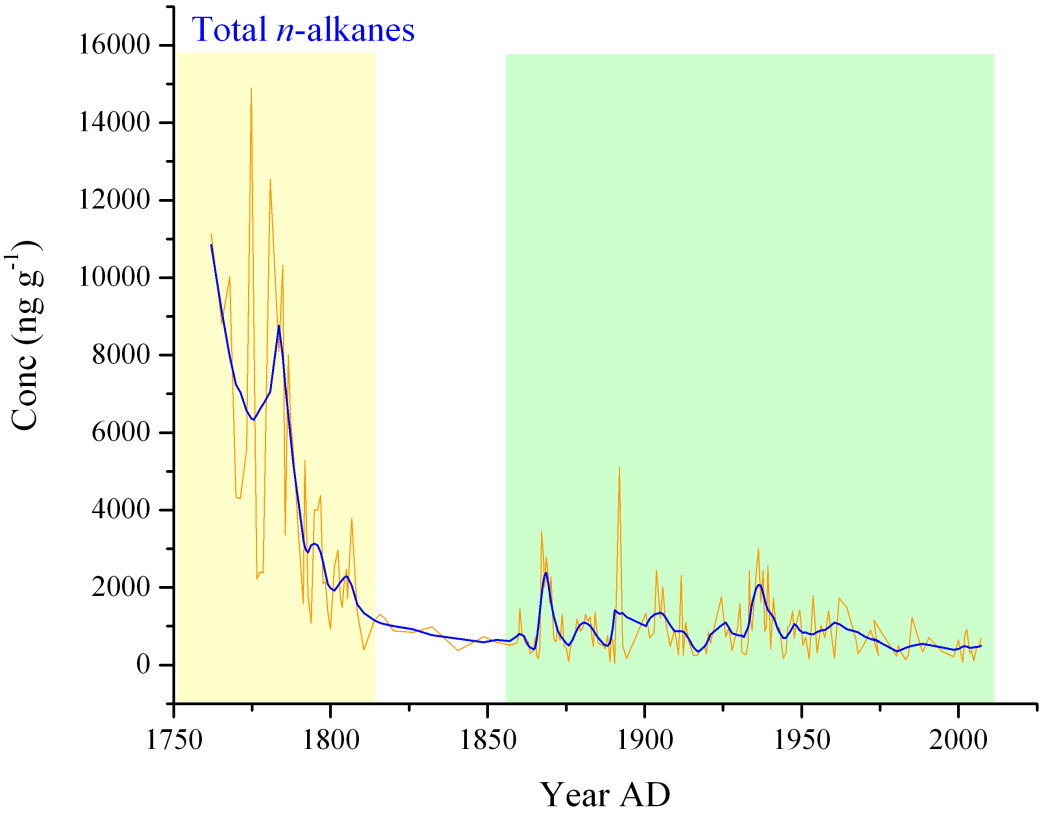

Figure 3.6. Total amount of *n*-alkanes (ng g^{-1}) preserved in the KNI-51-11 stalagmite.

The total amount of *n*-alkanes varies from a maximum of 171µg g^{-1} to a minimum value of 36 ng g^{-1}.

Looking at the yellow part of figure 3.6, the initial concentration of *n*-alkanes is high, and it decreases until around 1830. This tendency is probably related to the last phase of a phenomenon started before the formation of the stalagmite. In

contrast, the green part of fig. 3.6 shows a very irregular trend and the total amount of *n*-alkanes is significantly lower than at the beginning of the record.

Variations in the total *n*-alkanes concentration are driven by several factors and correspond to different changes in vegetation. These molecules are found primarily in leaf cuticle, which regulates water balance. Consequently, permeability and thickness of this layer respond to changes in temperature and humidity: plants adapt to drought conditions by increasing the cuticle to prevent water loss and conversely under more humid conditions [53]. Therefore, a variation in total *n*-alkane concentration may be related to plant adaptations to different climatic conditions. According to a study conducted in Northern Australia in both of the two dominant species, Acacia and Eucalyptus, the concentration of *n*-alkanes increases moving to warmer, drier areas, albeit by different orders of magnitude [54]. Therefore, an increase of the total amount of *n*-alkanes may be due to an increase in production of these compounds per single plant without variations in the abundance of individuals in the vegetation community. However, another interpretation of the high total amount of *n*-alkanes is the presence of a larger plant community that thrives in response to increased water availability. Thus, the total concentration results from the contributions of more individuals in the community. Furthermore, changes in the concentration of these molecules correspond to changes in vegetation cover [25] as shown in fig. 3.6: high amounts of *n*-alkanes indicate high and dense vegetation cover (yellow part in fig. 3.6), while lower concentrations of biomarkers indicate rarer vegetation (green part in fig. 3.6).

An important remark is that even though the vegetation above the cave consists primarily of Acacia and Eucalyptus, the analysis of *n*-alkanes does not identify single plant species because the molecules preserved in the stalagmite may originate from a variety of plant sources. These analyses are nonetheless important for reconstructing plant adaptations and hence past local climatic conditions.

3.3.1 Odd/even predominance

As previously mentioned, leaf waxes of terrestrial plants are characterized by a predominance of long odd chains of *n*-alkanes [23]. However, the samples analyzed in this study do not exhibit any predominance, as shown in fig. 3.7.

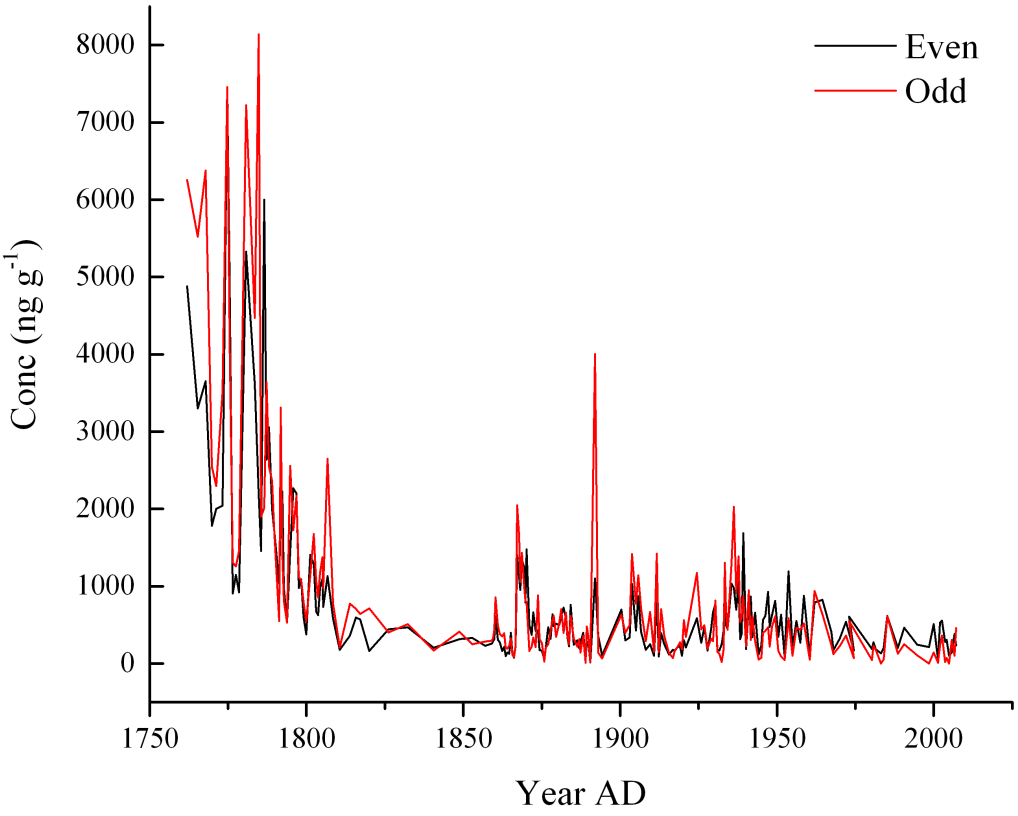

Figure 3.7. Distribution of odd and even *n*-alkanes chains present in the samples.

The lack of predominance is confirmed by the application of the Carbon Preference Index (CPI). This index measures the extent to which the distribution of *n*-alkane chains reflects the odd/even dominance typical of higher plants and it was calculated as follows [22]:

$$CPI = \frac{\sum_{odd} C_{25-33} + \sum_{odd} C_{27-35}}{2\sum_{even} C_{22-24}}$$

All terrestrial plants are characterized by CPI values greater than 1 (ranging from 5 to 10) as a result of the strong dominance of odd chains over even ones. CPI

values may decrease over time in response to microbial activity, recycled organic matter, or petroleum contamination (which can be excluded since the cave is located in a remote and pristine area) [13, 19]. In this case, CPI values range from a minimum of 0 to a maximum of 13. The variability of the results is consistent with fig. 3.7, hence supporting the lack of predominance between even and odd chains.

An important remark about the similarity of the distributions found in the samples is that the analyzed *n*-alkanes preserved in the stalagmite may have been altered by the action of various processes, starting with transport. Moreover, while the studied cave is located in Northern Australia, which is featured by the alternation of dry and wet seasons, most of the experiments on odd/even predominance have been carried out in the northern hemisphere in cold or temperate climates, with no dry periods, characterized by a great diversity of plant species and very different soil types [56]. A study conducted in Australia reports a dominance reversal between *n*-alkanes in plant tissues and those collected from the underlying soil [56]. More specifically, while leaves and roots of C3 and C4 plants show the characteristic prevalence of long odd chains, soil samples collected from both grasslands and forests show a strong dominance of short even chains. The same authors explain that the main sources of even short *n*-alkanes chains are C3 plants present in both forests and grasslands [56]. Another feature of the Australian vegetation is the strong dominance of C4 plants over C3, that appears to be favored by environmental conditions such as seasonal rainfall, drought and fire [57]. The two plant typologies use different photosynthetic pathways that may influence the distribution of *n*-alkane chains. Transport is another mechanism that could affect the lack of predominance found in this research. Little is still known about its selectivity and which features favor the movement of some molecules rather than others. Further research is needed to investigate how residence time, water properties, bedrock type, and other factors may discriminate or alter the compounds of the surface. Finally yet importantly, is the influence of microbial activity that will be further discussed in the next section.

3.3.2 Microbial activity

The *n*-alkanes preserved in the stalagmite may have been altered by the microbes living in the cave either by contributing to the input of organic matter with a different distribution of *n*-alkanes or by manipulating the odd chains already present [58]. Since both the cave and the overlying soil host microbial communities and there is no predominance of odd chains typical of higher plants, it is very likely that bacteria have altered the distribution of *n*-alkanes. A way to estimate the amount of reworked *n*-alkanes in the samples is to apply the index proposed by Villanueva et al. (1997) calculated as follows [58]:

$$A_r = C_{nr} - A_0$$

where A_r is the quantity of reworked *n*-alkanes, C_{nr} is the sum of homologues *n*-alkanes and A_0 is the total amount of *n*-alkanes produced by higher plants (not reworked).

C_{nr} has been calculated by applying this formula:

$$C_{nr} = \sum_{i=20}^{33} C_i$$

A_0 has been derived in two steps:

1. First, the total quantity of odd *n*-alkanes produced by higher plants $A_{(21+2i)}$ was calculated:

   $$A_{(21+2i)} = C_{(21+2i)} + \frac{C_{(22+2i)}+C_{(20+2i)}}{2} \quad with\ i \cong 1-6$$

   where $C_{(21+2i)}$ represents the concentration of each odd *n*-alkane
2. Second, A_0 was determined by applying this formula:

   $$A_0 = \sum_{i=1}^{6} A_{(21+2i)} = \sum_{i=1}^{6} C_{(21+2i)} - \sum_{i=1}^{6} C_{(22+2i)} - \frac{C_{22} + C_{32}}{2}$$

Villanueva et al. (1997) elaborated this index during their research work on North Atlantic Ocean cores and it was designed for marine ecosystems and terrestrial soils where no predominance is found among *n*-alkane chains [58]. The index, developed for soil samples, is applied for the first time to a stalagmite since the cave receives input of organic material from the overlying soil and, as

demonstrated for other caves [19, 20], hosts a microbial community, so the alteration of *n*-alkanes by bacteria is very likely.

Results are displayed below (negative values represent microbial inputs):

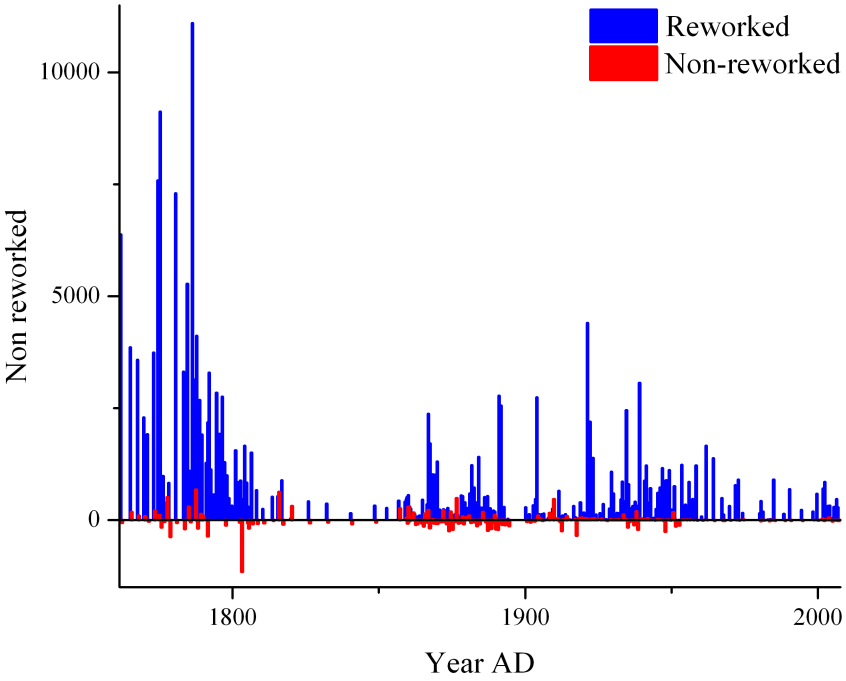

Figure 3.8. Comparison between unaltered and reworked *n*-alkanes preserved in the KNI-51-11 stalagmite.

Fig. 3.8 shows how almost all the *n*-alkanes have been altered by the microbial community. These results demonstrate the presence of bacteria that can alter the information preserved in the archives. Further research is needed to understand the extent and the intensity of microbial activity, which factors favor it, and to disentangle whether it is more present in the overlying soil or inside the cave.

3.3.3 Chain length

The length of *n*-alkane chains is another feature that requires further investigation as it reveals valuable information. While low-molecular-weight chains indicate bacterial activity [24], long *n*-alkane chains (25-35 carbon atoms) are abundant in the cuticle of terrestrial plants [22].

The distribution of *n*-alkane chains was further investigated by applying the Average Chain Length (ACL). This parameter is characteristic of *n*-alkane chains synthesized by higher plants and represents the weighted average of carbon atoms of several chain lengths [16, 10]. ACL was calculated with this formula:

$$ACL = \frac{\sum_{n=10}^{35}(C_n \times n)}{\sum C_n}$$

where C_n is the concentration of each *n*-alkane and *n* is the number of carbon atoms constituting the chain [10]. Figure 3.9 shows the ACL values determined for each sample.

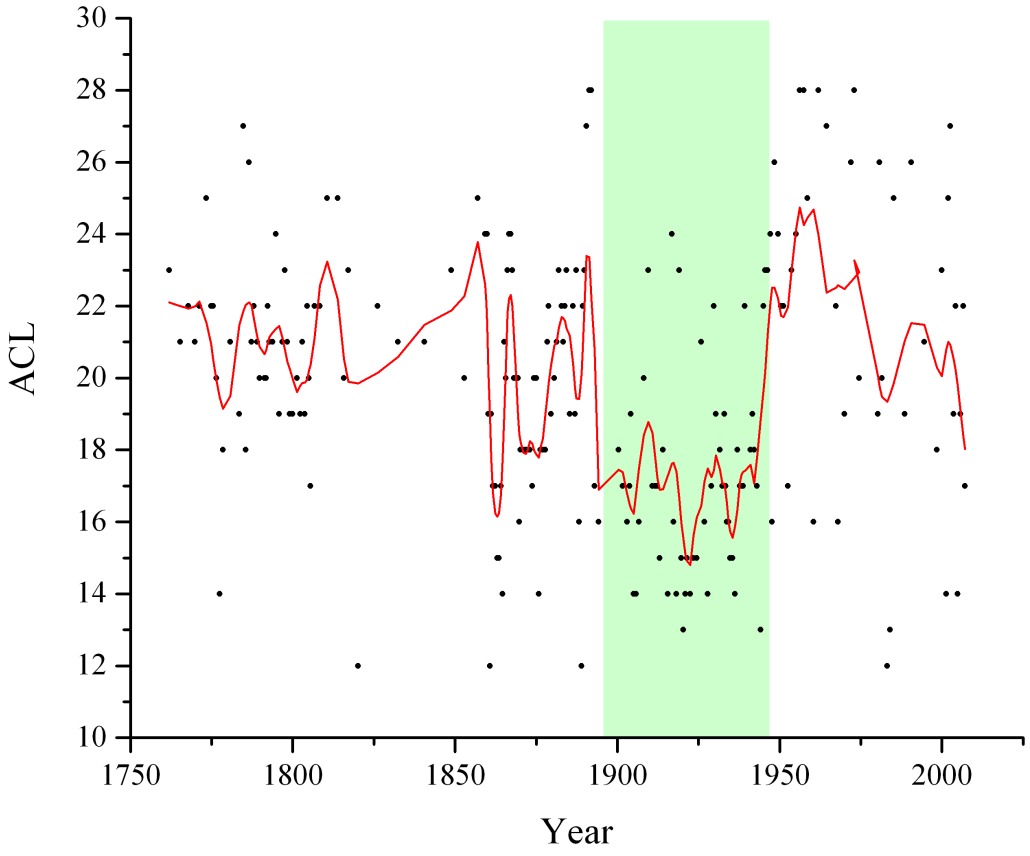

Figure 3.9. Trend of ACL values throughout the stalagmite growth.

High ACL values correspond to high concentrations of long *n*-alkane chains. This means that plants synthesize greater amounts of these molecules to thicken the cuticle and adapt to aridity. Dry conditions correspond to the period between 1950 and 1970 approximately. The green part in fig. 3.9 highlights low ACL values

indicating an increased production of short chains of *n*-alkanes by plants that could be a response to wet periods [10, 17]. The portions in which the ACL trend is regular coincide with periods in which fluctuations in *n*-alkane composition have limited amplitude: for instance, between about 1750 and 1800 ACL values range from 19 to 23. A study of several Australian ecosystems shows that soil samples exhibit different *n*-alkane distributions compared to local vegetation. Results show that biodegradation reduces CPI values (and thus affects the odd to even ratio of the chains) but does not significantly alter ACL values [62]. The researchers' hypothesis is that only a small fraction of *n*-alkanes found in the soil originates from local vegetation, since the largest contributions derive from past ecosystems and molecules transported over long distances by wind and water.

Clearly, the interpretation of ACL is complex as it is influenced by several factors. This index provides information on the change in plant response due to different climatic conditions: cuticle thickening (and therefore production of long *n*-alkane chains) is related to increased dryness [10, 19]. However, as the aforementioned study suggests, a complete interpretation of the ACL should consider, along with the climatic factor, other processes that may have altered the composition of *n*-alkane chains [62].

Another investigation was carried out to understand whether changes in ACL are due to species turnover in the plant community. Some researchers suggest to compare C29, C31 and C33 chain concentrations in samples to distinguish woody plants (featured by the abundance of C29) from grasses (where C31 and C33 chains prevail) [23]. The next figure displays the trends of these three *n*-alkane chains.

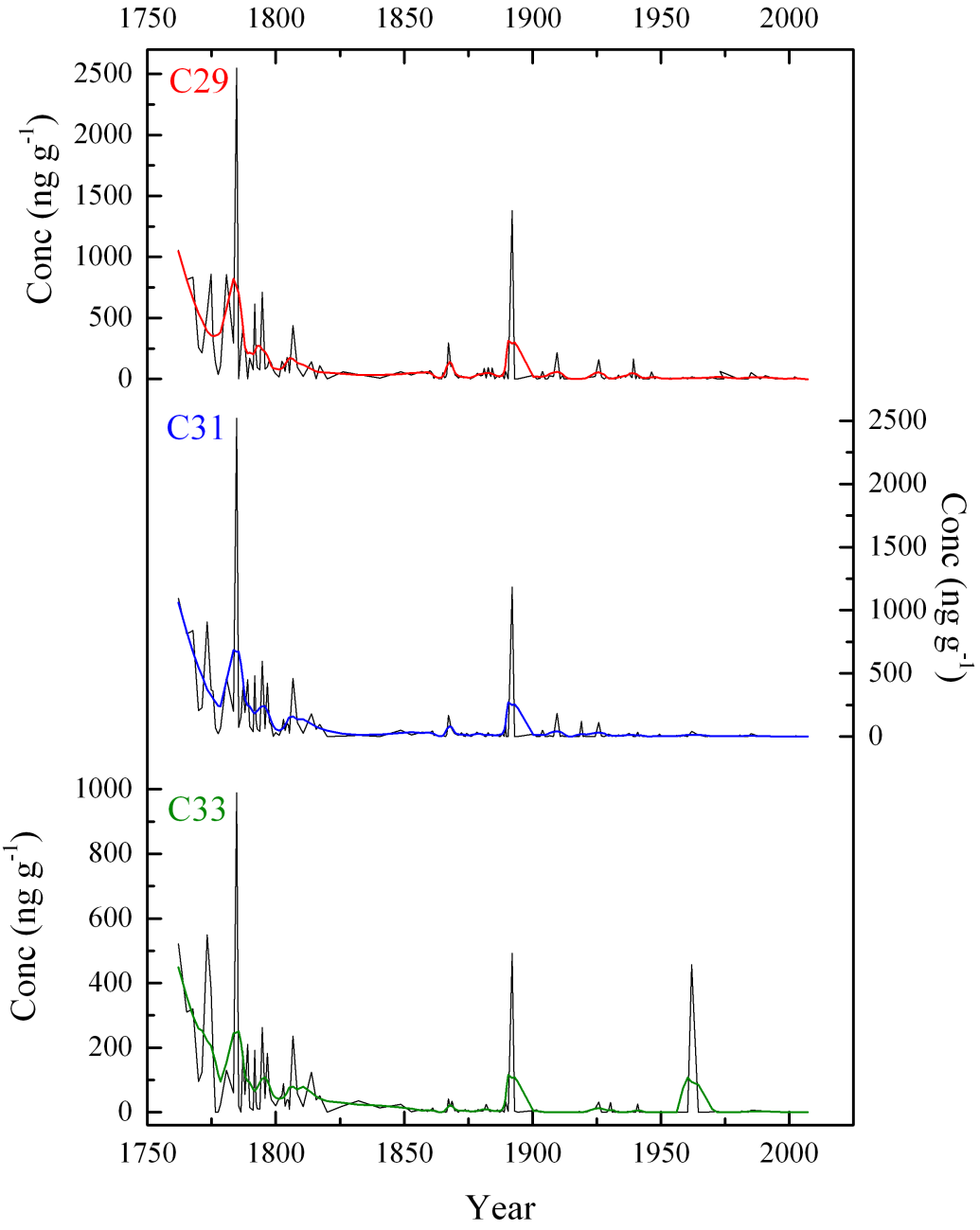

Figure 3.10. Concentrations of C29, C31 and C33.

As the three molecules show similar trends, it is very unlikely that species turnover occurred, so it is probable that ACL variations are not related to changes in the plant community, but rather to fire and land-use change.

Two other indices proposed by De la Rosa et al (2012) were used to better analyze the distribution of *n*-alkane chains. These parameters measure the relative abundance of short and long *n*-alkane chains present in the samples [63]. The two indices were calculated using these two formulas:

$$short/long = \frac{\sum_{i=10}^{23} C_i}{\sum_{i=24}^{33} C_i}$$

$$long/total = \frac{\sum_{i=24}^{33} C_i}{\sum_{i=10}^{33} C_i}$$

According to the authors, the predominance of short over long *n*-alkane chains is the result of biomass burning where high flame temperatures can cause the thermal breakdown of long *n*-alkanes chains, since they are the most thermolabile. As a result, the products of combustion show a higher short-to-long ratio consistent with the lack of predominance of long odd chains characteristic of higher plants [63]. Another research in Australia found an inverted long/short ratio between C4 and C3 plant tissues and underlying soil samples. The authors hypothesize that the inversion of distributions is due to fire as it selectively breaks long *n*-alkanes chains and consequently increases the short-to-long ratio in soil samples [56]. As for the current research, the vegetation above the cave consists primarily of Acacia and Eucalyptus and is often affected by bushfires, so fire is assumed to be one of the factors that altered the distribution of *n*-alkane chains. The next figure (fig. 3.11) summarizes all the indices used to examine *n*-alkane chains distributions.

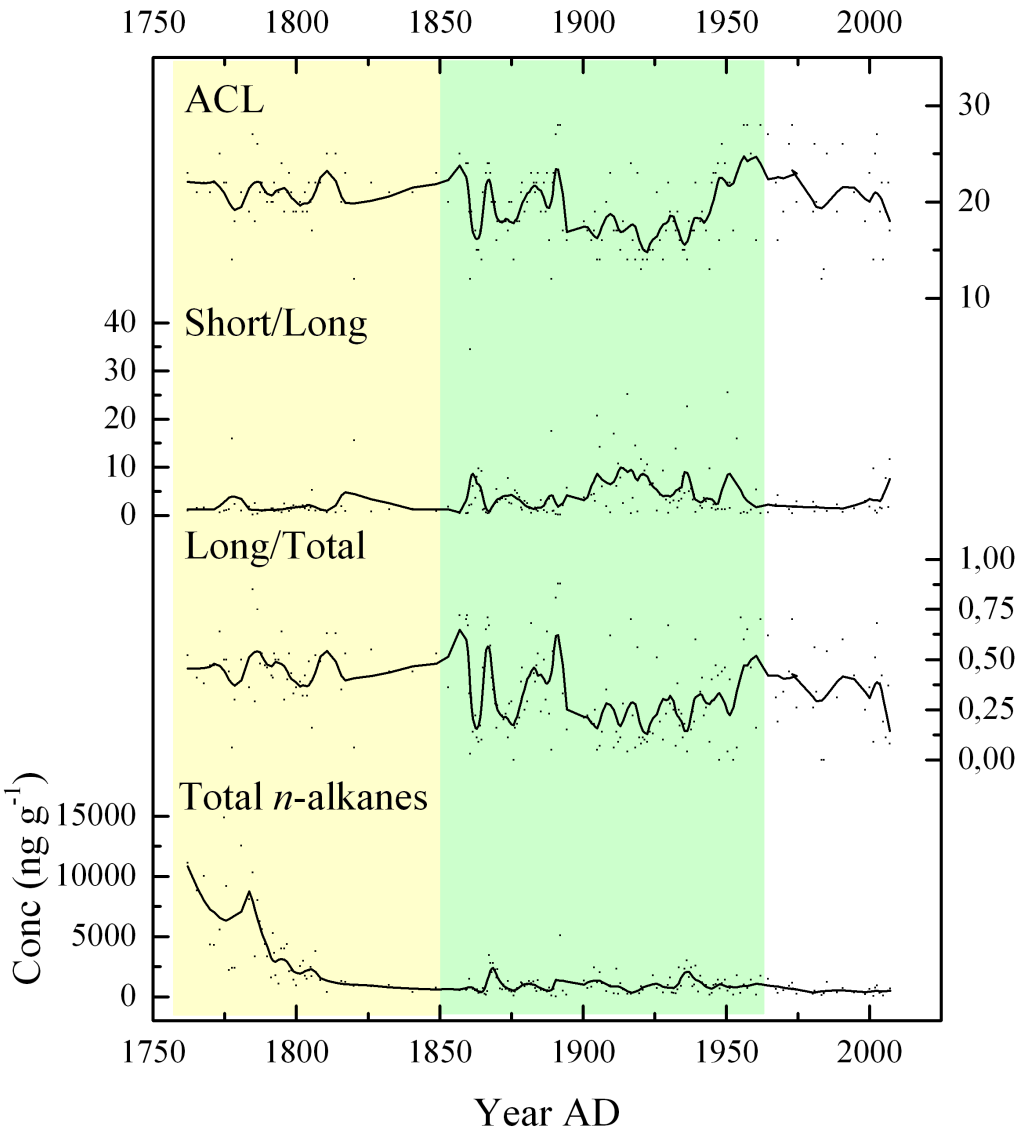

Figure 3.11. Summary of all indexes applied to *n*-alkane chain distributions.

The yellow rectangle in fig. 3.11 shows that ACL, short/long, and long/total are rather regular, meaning that the composition of *n*-alkanes is more or less constant over this period. At the same time, the total concentration decreases indicating a reduction in plant cover or a decrease in the production of these molecules as plants adaptation to wetter conditions. From approximately 1830 there is a gradual increase in ACL and long/total ratio while the short/long index decreases, and the total concentration has limited variations. Increased production of long *n*-alkane chains may correspond to a thickening of the cuticle as plant adaption to

drought conditions. From 1850 onwards, there are two sharp decreases in both the ACL and the long/total ratio, implying that the composition of *n*-alkanes is changing, as confirmed by the simultaneous increase in the short/long index. These abrupt changes may be explained by biomass burning, which causes thermal degradation of the long *n*-alkane chains and therefore increases the concentration of the short ones. Both ACL and long/total values start to increase again in 1950, but the latter do not reach values as high as at the beginning of the record.

3.4 MULTI-PROXY INTERPRETATION

The multi-proxy approach, employed in this research work, integrates several analyses so to provide a more comprehensive interpretation of fire history. The summary of key findings is shown in fig. 3.12.

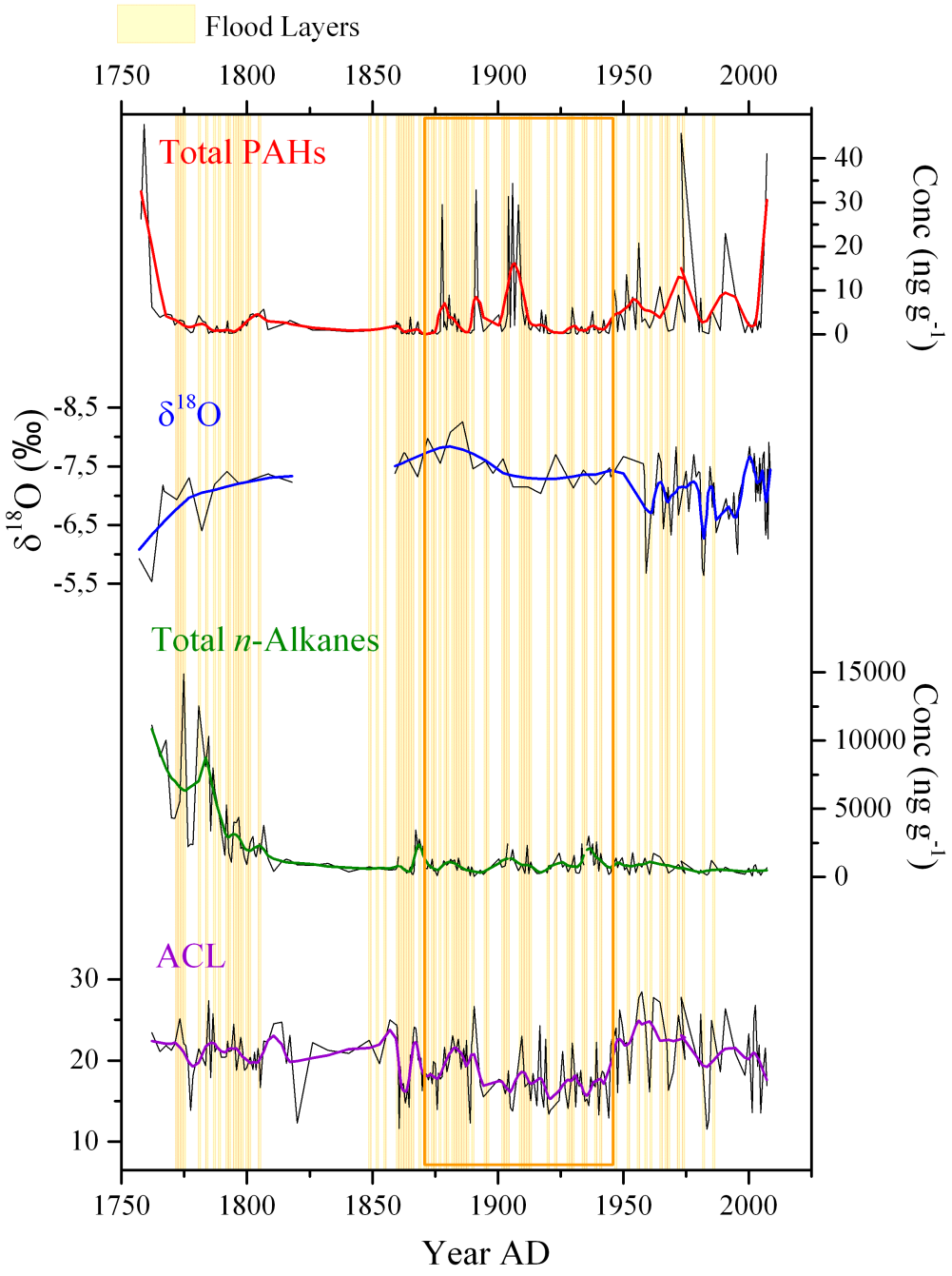

Figure 3.12. Main results of the present research work.
From the top: total amount of PAHs; $\delta^{18}O$; total concentration of *n*-alkanes; ACL index.
Background: mud layers.

Early in the record, between about 1750 and 1830, there is a sharp decrease in total PAHs and *n*-alkane concentrations that corresponds to decreasing $\delta^{18}O$ values while the ACL index remains mostly constant. This is probably the tail end of an event that began prior to the formation of the stalagmite. During this phase, a relationship between total PAHs, total *n*-alkanes and $\delta^{18}O$ is evident since they present similar trends. It is likely that natural fires occurred during this period as their intensity decreases with increasing humidity (as indicated by PAHs and $\delta^{18}O$ trends). The highest values of *n*-alkane concentrations are found only at the beginning of the record and they decrease steeply during this period. This trend can be explained by plant adaptations in response to increasing moisture. It is likely that plants have reduced cuticle thickness and thus limited the synthesis of *n*-alkanes per individual as a result of reduced drought. In fact, constant ACL values correspond to unvarying *n*-alkane composition and thus a shift in the plant community composition is unlikely.

Starting from approximately 1870, PAHs and $\delta^{18}O$ values are no longer correlated, so fire activity is independent from humidity conditions. Fires show a very different trend compared to the beginning of the record because they have greater intensity and frequency, as confirmed by the numerous peaks in PAH concentrations. Regarding the other proxies, the *n*-alkane trend does not show any relations with $\delta^{18}O$ values while the ACL index initially increases and after a sharp drop, it oscillates slightly on the lowest values of the record. These results reveal that while in earlier periods the amount of *n*-alkanes and ACL varied in response to climatic conditions, from 1870 onwards, the trend of these proxies is related to fire. According to a study conducted in Australia, fire selectively breaks down the long *n*-alkane chains and thus may alter ACL values [56]. Furthermore, other researchers have shown that fire unbalances the ratio of short to long chains of *n*-alkanes, favoring the short ones in combustion products [63]. In fig. 3.12, there is a lag in the peaks of *n*-alkanes compared to PAHs, from 1870 onwards that may correspond to a recovery of vegetation after a significant fire event. However, the delay may be the result of several factors such a different interaction between the molecules and the overlying soil or the stalagmite. PAHs

and *n*-alkanes are very different molecules in both size and chemical nature, and this may have an influence on the residence time and probably on the delay between peaks. Further research is needed to better understand how the different nature of PAHs and *n*-alkanes may lead to different interactions during transport and with the archive so to have a more accurate interpretation of the results.
From the 1950s onwards, fig. 3.12 displays a series of PAHs peaks unrelated to $\delta^{18}O$ values, corresponding to an increase in frequency and intensity of fire events unrelated to climatic conditions. The record ends with a rapid spike in PAHs concentration denoting a significantly greater extent of wildfires than any past event. During the same period, the total amount of *n*-alkanes reaches the lowest values, remaining more or less stable until the end of the record while ACL values show a sharp increase around 1950 and then slowly decline. These trends may indicate a variation in vegetation in response to fire activity and land use change.

The yellow lines in the background of fig. 3.12 represent the layers of mud included in the structure of the stalagmite as a result of numerous floods that occurred throughout its growth. The vertical section of the stalagmite presents a succession of white layers (aragonite) alternating with brown ones (mud). Further analysis was performed to understand if the presence of mud could affect the concentration of PAHs and *n*-alkanes in the samples, and if the rate of accumulation of these molecules in the mud was different from aragonite. Flood layer data were provided by Denniston et al. in collaboration with the National Centers for Environmental Information, NESDIS, NOAA, U.S. Department of Commerce [64].
Calculations of the correlation between biomarker concentrations and mud layers did not yield significant results, so no evident relationship is present between mud layers and variations in PAH and *n*-alkane concentrations. This is consistent with data shown in fig. 3.12: the overlap between the main proxies of this study and mud layers shows that there is no evident correspondence between PAHs or *n*-alkanes peaks and flood frequency. Results demonstrate that the accumulation rate of PAHs and *n*-alkanes remains unchanged between mud and aragonite so it is

likely that the deposition of these biomarkers is not affected by the presence of mud layers. However, as this field of research is in its early stages, further investigation is needed to understand if there is any relation between the variations in PAHs and *n*-alkanes concentrations in the stalagmite and flood frequency and what other factors influence the sedimentation of these organic compounds.

3.5 IMPACT OF THE EUROPEAN COLONIZATION

It is interesting to note that the unequivocal increase in fire frequency and intensity occurred concurrently with the European colonization. Indeed, pastoral settlement began in the Kimberley in the 1880s and it coincided with the rapid eradication of the Aboriginal population causing the decline of fire practices and significant changes among plant and animal communities [65]. As previously discussed in 3.4, the increase in fire intensity and frequency from the 1870s reflects the enormous difference in fire management between Aboriginals and Europeans. The former frequently burned the land with small fires to reduce the amount of grass and wood that could become fuel for potential extreme events [9, 10]. They had a deep knowledge of how to manage fires, as they were part of their culture and a crucial survival tool. Fire was a way to obtain resources from the surrounding environment, a means of communicating the occupation of a territory, but also a form of defence against white people [65]. Europeans, on the other hand, were mostly farmers who needed to expand meadows and pastures so their practices consisted of rare but very intense fires that sometimes over-extended [50].

The fire regime recorded from the late 1800s presumably has an anthropogenic origin because the PAHs pattern is independent of climatic conditions (as displayed by $\delta^{18}O$ values) and is very different from earlier periods in terms of frequency and intensity. Moreover, trends in *n*-alkanes and ACL are also not related to variations in humidity. This change could be the result of the European colonization for several reasons, first of all the coincidence between their arrival

in Northern Australia and the beginning of a new phase of fires. In fact, since the late 1800s, there has been a pronounced increase in fire intensity and frequency that is unprecedented in the record. Therefore, to better understand this trend, the fire regime recorded by stalagmite KNI-51-11 was compared to that of a stalagmite previously grown in the same cave and subjected to the same type of analysis (stalagmite KNI-11-F) [66]. The comparison reveals that frequency and intensity of fires from the end of 1800 is significantly greater than all the peaks of the stalagmite KNI-51-F indicating that a sudden change of this magnitude has never been recorded before [66]. Moreover, fire activity is matched by plant adaptations whose changes are no longer related to climatic conditions, but are in response to fire, as indicated by *n*-alkane and ACL trends.

The distinction between natural fires at the beginning of the record and anthropogenic fires (post-1870) is clearly visible in fig.3.12: while the former have a trend related to humidity conditions, the latter are characterized by peaks with frequency and intensity very different from past periods and are independent of climatic conditions. The anthropogenic impact is more evident from the '50s. The series of peaks is even followed by an abrupt and rapid increase in fire activity from the 2000s. A historical datum of considerable importance for assessing the anthropogenic effect is the founding of the Kununurra town in 1961, which corresponds to a significant peak in PAHs concentration, as expected. Moreover, from approximately the 1950s onward, ACL values and total *n*-alkane concentration gradually decrease and no longer reach values as high as at the beginning of the record indicating a probable land-use change resulting from urbanization and a consequent shift in the plant community. This demonstrates the validity of the stalagmite as a paleoclimatic archive because it recorded an event traceable by historical data. However, a further test of the reliability of the record would be to compare the data achieved in this research with other archives covering the same period. This was not feasible due to the lack of high-resolution charcoal and pollen data, so it was not possible to provide a more accurate reconstruction of the plant community changes that occurred in each period.

In the last part of the record, starting in the 2000s, the spike in PAHs concentration is clearly visible, indicating an abrupt and rapid increase in fire activity and corresponding to events of considerably greater size and intensity than in the past. According to a study conducted in Northern Australia, today the Kimberley region is sparsely inhabited, half of the territory is used for pastoralism and the remaining half is an Aboriginal reserve [65]. As for fires, local authorities prohibit the use of fire from the beginning of the dry season (April 1) and create firebreaks to prevent the expansion of potential fires. Nowadays fire is used by Aborigines to hunt and remove dry grasses and wood (and thus preventing extreme events) and by shepherds to improve soil fertility. The end of the dry season is the most critical period in terms of uncontrolled wildfires, whose extent varies from year to year, continuously monitored by satellites. The same authors, comparing modern and historical data, found a general increase in fires, particularly at the beginning of the dry season. This is consistent with fire prevention promoted by local authorities that encourage small fires at the beginning of the dry season to avoid uncontrolled phenomena at the end of the same season [65]. The overall increase in fires found in this study is reflected in the spike in PAH concentrations over the last few decades of the record, as seen in fig. 3.12.

Since the analyzed record covers a historical period in which fire data are available from different sources, PAH results were qualitatively compared with satellite maps of fire scars from the Northern Australian Fire Information (NAFI) covering the last decade of the record and shown in the next figure.

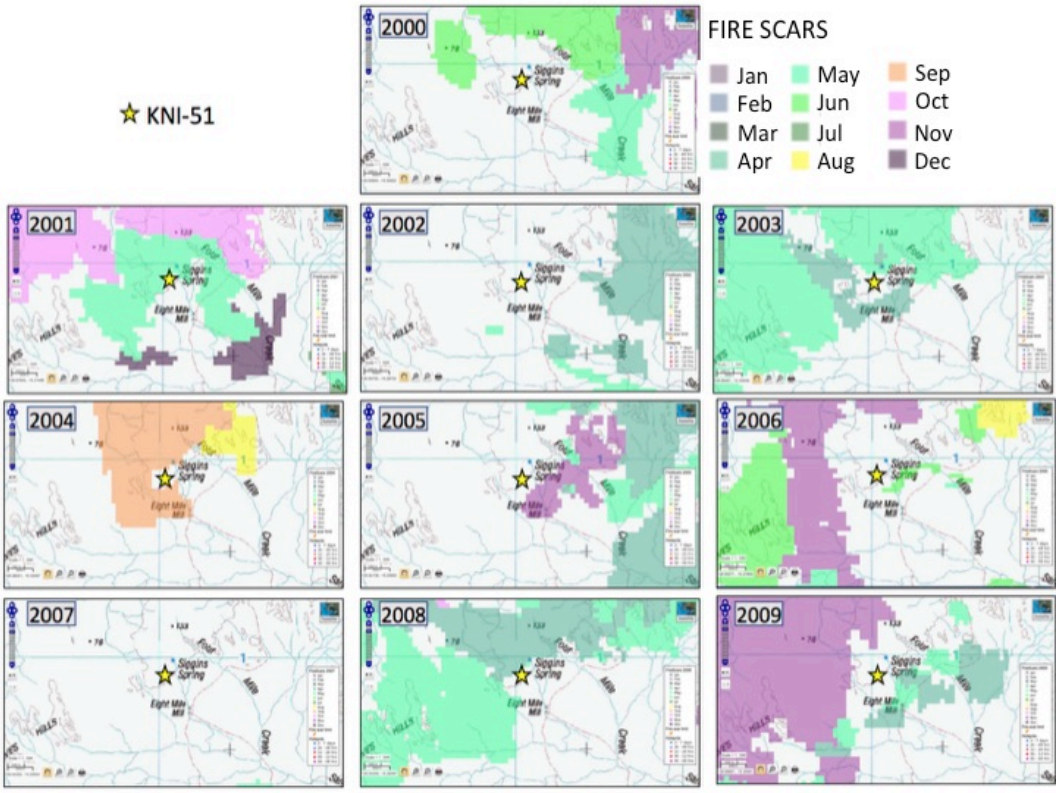

Figure 3.13. Satellite maps from 2000 to 2009 showing burned areas in the surroundings of the cave KNI-51 [67].

Every color in fig. 3.13 represents the area burned in each month. According to the maps above, the greatest extent of fires occurred in the years 2001, 2003, and 2008. The most affected months by bushfires are June, July, and November, although in some years fires have occurred in May, August, and September. Some fires have likely burned the land above the cave, particularly in the years 2001, 2003, and 2008. This qualitative interpretation of the satellite maps is consistent with trends in PAH concentrations over the last decade of the record where the spike in fire activity is clearly visible and indicates events of greater intensity and extent than in the past.

Comparing fire proxies recorded from the stalagmite with historical and satellite data further highlights the high significance of the record in tracking past fire events.

4. CONCLUSIONS

This research work aimed at reconstructing the history of fires over the last three hundred years through the analysis of trace organic compounds preserved in the stalagmite KNI-51-11. The present work is part of an emerging field of research, in which the few available studies report only low-resolution results. The analytical approach applied here is very innovative because PAHs are used for the first time as fire proxy in speleothems, providing high-resolution information on the intensity and frequency of fire events. Even though this is an exploratory survey, results show that PAHs found in speleothems can be used as valuable fire proxies for future investigations in this promising field of research. As this was a multi-proxy approach, the PAHs data were correlated with those of *n*-alkanes extracted through the same procedure and with $\delta^{18}O$ record, providing a more comprehensive interpretation of the results. The integration of fire, vegetation, and climate proxies employed in this work supports the use of PAHs as proxy for the reconstruction of past fire events, that is extremely important for better predicting future fires and improving land management and community readiness.

The analyzed record reveals the difference between natural fires that occurred in the first century of the record and anthropogenic fires that began in the late 1800s, concurrent with the arrival of Europeans. Indeed, while the former are closely linked to climatic conditions, the latter show a significant increase in intensity and frequency independent from aridity and humidity. The record ends with a strong increase in fire events with unprecedented extent and frequency, most likely due to anthropogenic impact. These findings are consistent with *n*-alkane data indicating that in the first century plant adaptations are driven by climatic conditions and from the end of 1800 onwards they are in response to fire.
Comparing the results with historical and satellite data demonstrates the validity of the stalagmite as a significant paleoclimatic archive because it recorded past events comparable to other sources. Furthermore, analyses of *n*-alkanes reveal the lack of odd-even predominance typical of higher plants likely attributable to the

microbial alteration occurring on the soil and within the cave. The increase in the ratio of short to long chains around the late 1800s may be the result of increased fire events causing thermal degradation of the long chains. Lastly, trends in *n*-alkanes and ACLs from approximately 1950 onwards suggest variations in the plant community in response to fire activity and land use change as a consequence of urbanization.

This work raises additional questions for future research. The role and extent of microbial alteration should be further investigated because little is still known about the contribution of soil and cave communities. Further research is needed on the mediation of calcite precipitation by bacteria and the extent of this phenomenon. Moreover, the understanding of transport selectivity should be improved along with influencing factors and favored molecules. A more comprehensive knowledge of speleothems and how the climate signal is recorded is essential for their use in paleoclimatic reconstructions and it certainly broadens the areas of investigation.

5. REFERENCES

[1] A. H. Lynch *et al.*, "Using the Paleorecord to Evaluate Climate and Fire Interactions in Australia," *Annu. Rev. Earth Planet. Sci.*, vol. 35, no. 1, pp. 215–239, 2007.

[2] A. Spessa, B. McBeth, and C. Prentice, "Relationships among fire frequency, rainfall and vegetation patterns in the wet-dry tropics of northern Australia: An analysis based on NOAA-AVHRR data," *Glob. Ecol. Biogeogr.*, vol. 14, no. 5, pp. 439–454, 2005.

[3] T. He, B. B. Lamont, and J. G. Pausas, "Fire as a key driver of Earth's biodiversity," *Biol. Rev.*, vol. 94, no. 6, pp. 1983–2010, 2019.

[4] Australian Government, "Our natural environment." [Online]. Available: https://www.australia.gov.au/about-australia/our-country/our-natural-environment. [Accessed: 16-Mar-2020].

[5] Bureau of Meteorology, "Bushfire weather." [Online]. Available: http://www.bom.gov.au/weather-services/fire-weather-centre/bushfire-weather/index.shtml. [Accessed: 16-Mar-2020].

[6] The Guardian Australia, "Bushfire crisis conditions eight times more likely under 2C warming, analysis shows." [Online]. Available: https://www.theguardian.com/australia-news/2020/mar/05/bushfire-crisis-conditions-eight-times-more-likely-under-2c-warming-analysis-shows. [Accessed: 17-Mar-2020].

[7] F. Times, "Australia's PM refuses to change climate policy after deadly fires." [Online]. Available: https://www.ft.com/content/0a499264-2482-11ea-9a4f-963f0ec7e134. [Accessed: 21-Oct-2020].

[8] William F. Ruddiman, *Earth's Climate: Past and Future*, Third Edit. W. H. Freeman and Company, New York, 2013.

[9] NOAA, "What Are 'Proxy' Data?" [Online]. Available: https://www.ncdc.noaa.gov/news/what-are-proxy-data. [Accessed: 18-Mar-2020].

[10] N. Dubois and J. Jacob, "Molecular biomarkers of anthropic impacts in natural archives: A review," *Front. Ecol. Evol.*, vol. 4, no. AUG, pp. 1–16, 2016.

[11] T. E. McGrath, W. G. Chan, and R. Hajajigol, "Low temperature mechanism for the formation of polycyclic aromatic hydrocarbons from the pyrolysis of cellulose. Journal of Analytical and Applied Pyrolysis, v. 66, p. 51-70, 2003.," *J. Anal. Appl. Pyrolysis*, vol. 66, pp. 51–70, 2003.

[12] Information National Centre for Environmental, "What Are Proxy Data?" [Online]. Available: https://www.ncei.noaa.gov/news/what-are-proxy-data. [Accessed: 21-Oct-2020].

[13] S. A. Elias and R. S. Bradley, *Paleoclimatology: Reconstructing Climates of the Quaternary*, vol. 31, no. 3. 1999.

[14] J. Hellstrom, "U-Th dating of speleothems with high initial 230Th using stratigraphical constraint," *Quat. Geochronol.*, vol. 1, no. 4, pp. 289–295, 2006.

[15] E. Argiriadis *et al.*, “Lake sediment fecal and biomass burning biomarkers provide direct evidence for prehistoric human-lit fires in New Zealand,” *Sci. Rep.*, vol. 8, no. 1, pp. 2–10, 2018.
[16] K. Ravindra, R. Sokhi, and R. Van Grieken, “Atmospheric polycyclic aromatic hydrocarbons: Source attribution, emission factors and regulation,” *Atmos. Environ.*, vol. 42, no. 13, pp. 2895–2921, 2008.
[17] A.-P. H. Statement, “ATSDR - Public Health Statement: Polycyclic Aromatic Hydrocarbons (PAHs).” [Online]. Available: https://www.atsdr.cdc.gov/phs/phs.asp?id=120&tid=25. [Accessed: 28-Jul-2020].
[18] J. C. Fetzer, “Large Polycyclic Aromatic Hydrocarbons: Chemistry and Analysis,” *Wiley-Interscience*, 2000. [Online]. Available: https://books.google.it/books?hl=it&lr=&id=X6NpmLR5FnwC&oi=fnd&pg=PR9&dq=polycyclic+aromatic+hydrocarbons+pah+book&ots=Gy9LTpCV-a&sig=PQHnmw15soyjdOg8dldbGYcMstE#v=onepage&q=polycyclic aromatic hydrocarbons pah book&f=false. [Accessed: 29-Jul-2020].
[19] E. Argiriadis and B. Carlo, “The Early Impact of Agriculture,” pp. 1–150, 2016.
[20] M. A. Nič M, Jirát J, Košata B, Jenkins A, “The IUPAC Compendium of Chemical Terminology,” *Research Triagle Park, NC*, 2009. [Online]. Available: https://goldbook.iupac.org/. [Accessed: 28-Jul-2020].
[21] P. T. Brown WH, “Introduction to Organic Chemistry,” *Wiley*, 2015. [Online]. Available: https://books.google.it/books?id=LhuRCgAAQBAJ&printsec=frontcover&dq=principles+of+organic+chemistry+Brown+WH&hl=it&sa=X&ved=2ahUKEwjcnvL68e_qAhW-VRUIHTl9DJEQ6AEwAXoECAAQAg#v=onepage&q&f=false. [Accessed: 28-Jul-2020].
[22] K. H. Freeman and R. D. Pancost, *Biomarkers for Terrestrial Plants and Climate*, 2nd ed., vol. 12. Elsevier Ltd., 2013.
[23] R. T. Bush and F. A. McInerney, “Leaf wax n-alkane distributions in and across modern plants: Implications for paleoecology and chemotaxonomy,” *Geochim. Cosmochim. Acta*, vol. 117, pp. 161–179, 2013.
[24] R. D. Pancost, M. Baas, B. Van Geel, and J. S. Sinninghe Damsté, “Biomarkers as proxies for plant inputs to peats: An example from a sub-boreal ombrotrophic bog,” *Org. Geochem.*, vol. 33, no. 7, pp. 675–690, 2002.
[25] I. D. Bull, P. F. V. Bergen, C. J. Nott, P. R. Poulton, and R. P. Evershed, “Organic geochemical studies of soils from the Rothamsted classical experiments - V. The fate of lipids in different long-term experiments,” *Org. Geochem.*, vol. 31, no. 5, pp. 389–408, 2000.
[26] A. J. Blyth, A. Asrat, A. Baker, P. Gulliver, M. J. Leng, and D. Genty, “A new approach to detecting vegetation and land-use change using high-resolution lipid biomarker records in stalagmites,” *Quat. Res.*, vol. 68, no. 3, pp. 314–324, 2007.
[27] A. J. Blyth, A. Hartland, and A. Baker, “Organic proxies in speleothems –

New developments, advantages and limitations," *Quat. Sci. Rev.*, vol. 149, pp. 1–17, 2016.
[28] R. S. Bradley, "Speleothems," *Paleoclimatology*, vol. 295, pp. 291–318, 2015.
[29] H. Schwarcz, "Stable Isotope Systematics in Speleothems," *Encycl. Quat. Sci.*, no. 1989, pp. 3215–3221, 2007.
[30] I. J. Fairchild *et al.*, "Modification and preservation of environmental signals in speleothems," *Earth-Science Rev.*, vol. 75, no. 1–4, pp. 105–153, 2006.
[31] V. J. Polyak and R. F. Denniston, *Paleoclimate Records from Speleothems*, Second Edi. Elsevier Inc., 2012.
[32] A. J. Blyth *et al.*, "Molecular organic matter in speleothems and its potential as an environmental proxy," *Quat. Sci. Rev.*, vol. 27, no. 9–10, pp. 905–921, 2008.
[33] F. Gázquez, J. M. Calaforra, P. Forti, H. Stoll, B. Ghaleb, and A. Delgado-Huertas, "Paleoflood events recorded by speleothems in caves," *Earth Surf. Process. Landforms*, vol. 39, no. 10, pp. 1345–1353, 2014.
[34] R. F. Denniston and M. Luetscher, "Speleothems as high-resolution paleoflood archives," *Quat. Sci. Rev.*, vol. 170, pp. 1–13, 2017.
[35] K. Ramseyer, T. M. Miano, V. D'Orazio, A. Wildberger, T. Wagner, and J. Geister, "Nature and origin of organic matter in carbonates from speleothems, marine cements and coral skeletons," *Org. Geochem.*, vol. 26, no. 5–6, pp. 361–378, 1997.
[36] V. J. Polyak and R. F. Denniston, *Paleoclimate Records from Speleothems*, Second Edi. Elsevier Inc., 2012.
[37] Y. Perrette *et al.*, "Polycyclic Aromatic Hydrocarbons in stalagmites: Occurrence and use for analyzing past environments," *Chem. Geol.*, vol. 251, no. 1–4, pp. 67–76, 2008.
[38] E. Argiriadis, R. F. Denniston, and C. Barbante, "Improved Polycyclic Aromatic Hydrocarbon and n-Alkane Determination in Speleothems through Cleanroom Sample Processing," *Anal. Chem.*, vol. 91, no. 11, pp. 7007–7011, 2019.
[39] Australian Bureau of Statistics, "Australia's climate," *Year B. Aust.*
[40] Google Maps, "Position of the cave KNI-51: 15°18'00.0"S 128°37'00.0"E." [Online]. Available: https://www.google.it/maps/place/15°18'00.0%22S+128°37'00.0%22E/@-15.2999948,110.6869754,5401457m/data=!3m1!1e3!4m6!3m5!1s0x0:0x0!7e2!8m2!3d-15.3!4d128.6166667. [Accessed: 22-Mar-2021].
[41] R. F. Denniston *et al.*, "A Stalagmite record of holocene indonesian-australian summer monsoon variability from the australian tropics," *Quat. Sci. Rev.*, vol. 78, pp. 155–168, 2013.
[42] R. F. Denniston *et al.*, "Extreme rainfall activity in the Australian tropics reflects changes in the El Niño/Southern Oscillation over the last two millennia.," *Proc. Natl. Acad. Sci. U. S. A.*, vol. 112, no. 15, pp. 4576–4581, Apr. 2015.
[43] Bureau of Meteorology, "What is a Tropical Cyclone?" [Online].

Available: http://www.bom.gov.au/cyclone/tropical-cyclone-knowledge-centre/understanding/tc-info/. [Accessed: 19-Oct-2020].
[44] Bureau of Meteorology, "What is the monsoon?" [Online]. Available: http://media.bom.gov.au/social/blog/2009/askbom-what-is-the-monsoon/. [Accessed: 19-Oct-2020].
[45] Bureau of Meteorology, "What is El Niño and what might it mean for Australia?" [Online]. Available: http://www.bom.gov.au/climate/updates/articles/a008-el-nino-and-australia.shtml. [Accessed: 19-Oct-2020].
[46] Bureau of Meteorology, "What is a La Niña?" [Online]. Available: http://media.bom.gov.au/social/blog/2440/explainer-what-is-a-la-nia/. [Accessed: 21-Oct-2020].
[47] I. Cresswell and H. Murphy, "Altered fire regimes," *Australia State of the Environment*, 2016. [Online]. Available: https://soe.environment.gov.au/theme/overview. [Accessed: 23-Sep-2020].
[48] D. Hinchley, O. Manager, and R. Woods, "How humans have impacted Australia's nature over time," *The Nature Conservacy Australia*, 2019. [Online]. Available: https://www.natureaustralia.org.au/what-we-do/our-insights/perspectives/human-impact-nature-australia/. [Accessed: 22-Sep-2020].
[49] E. O'Gorman, J. Beattie, and M. Henry, "Histories of climate, science, and colonization in Australia and New Zealand, 1800–1945," *Wiley Interdiscip. Rev. Clim. Chang.*, vol. 7, no. 6, pp. 893–909, 2016.
[50] S. E. Connor *et al.*, "Forgotten impacts of European land-use on riparian and savanna vegetation in northwest Australia," *J. Veg. Sci.*, vol. 29, no. 3, pp. 427–437, 2018.
[51] University of Newcastle Blog | UON Australia, "What makes Australian bushfires so dangerous?" [Online]. Available: https://blogs.newcastle.edu.au/blog/2013/10/22/what-makes-australian-bushfires-so-dangerous/. [Accessed: 21-Oct-2020].
[52] M. Hajaligol, B. Waymack, and D. Kellogg, "Low temperature formation of aromatic hydrocarbon from pyrolysis of cellulosic materials," *Fuel*, vol. 80, no. 12, pp. 1799–1807, 2001.
[53] M. Riederer and L. Schreiber, "Protecting against water loss: Analysis of the barrier properties of plant cuticles," *J. Exp. Bot.*, vol. 52, no. 363, pp. 2023–2032, 2001.
[54] B. Hoffmann, A. Kahmen, L. A. Cernusak, S. K. Arndt, and D. Sachse, "Abundance and distribution of leaf wax n-alkanes in leaves of acacia and eucalyptus trees along a strong humidity gradient in Northern Australia," *Org. Geochem.*, vol. 62, pp. 62–67, 2013.
[55] W. L. Jeng, "Higher plant n-alkane average chain length as an indicator of petrogenic hydrocarbon contamination in marine sediments," *Mar. Chem.*, vol. 102, no. 3–4, pp. 242–251, 2006.
[56] T. K. Kuhn, E. S. Krull, A. Bowater, K. Grice, and G. Gleixner, "The occurrence of short chain n-alkanes with an even over odd predominance in higher plants and soils," *Org. Geochem.*, vol. 41, no. 2, pp. 88–95, 2010.

[57] J. W. Andrae *et al.*, “Initial Expansion of C4 Vegetation in Australia During the Late Pliocene,” *Geophys. Res. Lett.*, vol. 45, no. 10, pp. 4831–4840, 2018.
[58] J. Villanueva, J. O. Grimalt, E. Cortijo, L. Vidal, and L. Labeyrie, “A biomarker approach to the organic matter deposited in the North Atlantic during the last climatic cycle,” *Geochim. Cosmochim. Acta*, vol. 61, no. 21, pp. 4633–4646, 1997.
[59] S. Bindschedler, G. Cailleau, and E. Verrecchia, “Role of fungi in the biomineralization of calcite,” *Minerals*, vol. 6, no. 2, pp. 1–19, 2016.
[60] S. Sanchez-Moral, J. C. Cañaveras, L. Laiz, C. Saiz-Jimenez, J. Bedoya, and L. Luque, “Biomediated precipitation of calcium carbonate metastable phases in hypogean environments: A short review,” *Geomicrobiol. J.*, vol. 20, no. 5, pp. 491–500, 2003.
[61] B. R. T. Simoneit, G. Sheng, X. Chen, J. Fu, J. Zhang, and Y. Xu, “Molecular marker study of extractable organic matter in aerosols from urban areas of China,” *Atmos. Environ. Part A, Gen. Top.*, vol. 25, no. 10, pp. 2111–2129, 1991.
[62] S. Howard, F. A. McInerney, S. Caddy-Retalic, P. A. Hall, and J. W. Andrae, “Modelling leaf wax n-alkane inputs to soils along a latitudinal transect across Australia,” *Org. Geochem.*, vol. 121, pp. 126–137, 2018.
[63] J. M. De la Rosa *et al.*, “Characterization of wildfire effects on soil organic matter using analytical pyrolysis,” *Geoderma*, vol. 191, pp. 24–30, 2012.
[64] R. F. Denniston *et al.*, “Cave KNI-51, Western Australia 2,200 Year Stalagmite Flood Layer Data,” 2015. [Online]. Available: https://www.ncdc.noaa.gov/paleo-search/?dataTypeId=18%0Ahttps://www.ncdc.noaa.gov/paleo-search/?dataTypeId=18%0Ahttps://www.ncdc.noaa.gov/paleo-search/study/2562. [Accessed: 23-Feb-2021].
[65] T. Vigilante, “Analysis of explorers’ records of Aboriginal landscape burning in the Kimberley region of Western Australia,” *Aust. Geogr. Stud.*, vol. 39, no. 2, pp. 135–155, 2001.
[66] M. Baltieri, D. Battistel, R. F. Denniston, and E. Arigiriadis, “RECONSTRUCTING FIRE HISTORY FROM STALAGMITE ORGANIC COMPOUNDS : A HIGH RESOLUTION STUDY FROM NORTHWESTERN,” 2019.
[67] NAFI, “Northern Australian & Rangelanders Fire Information.” [Online]. Available: https://firenorth.org.au/nafi3/. [Accessed: 09-Mar-2021].

6. ACKNOWLEDGEMENTS

I would like to thank with all my heart, Elena Argiriadis for all the endless support, patience and encouragement she has shown me, as well as for the passion she has transmitted to me throughout the time we shared. Despite all the unforeseen events… we made it!

A sincere thank you to Prof. Carlo Barbante and Prof. Rhawn Denniston for giving me the opportunity to challenge myself in the lab and for making this thesis possible.

A special thanks to the unstoppable Mara: without your help we would have never been able to finish the analysis of the samples and without your jokes and your useful advice the work would have been heavier.

I want to thank all the third floor of the Delta building and in particular Fabiana and Beatrice especially for the summer support and the delicious coffee breaks, along with Matteo and Giuliano for always cheering up the lunch hour.

I would like to thank my family for supporting and encouraging me. You gave me a wonderful opportunity to challenge myself and you strongly believed in me and in my potential. Thank you mom, dad, Ale and Renata. A very special thank you to my grandmother Pia who is so patient, listening and advising me every day.

This project would never have come to an end without the constant monitoring of Aleph: thank you for having adequately safeguarded it!

Thanks to Denis, who from faraway Melbourne was a vital help in revising the thesis and for various life advices, at any time of the day or night.

I do not want to forget Mohsen, Melika and Sumaia, amazing friends with whom I shared the efforts of the university but also the exciting life in Mestre.

Thanks to Airin, Simone, Cecilia, Ivan, Claudia from Kouvola, Yurina from Yokohama, Sandra and Anna for always being there beyond any distance and for making me smile.

Since I cannot list everyone, I want to thank those who have taught me, in very different ways, that every failure is an opportunity to reflect, get back up, and start over, stronger than before.